

## Nonsteroidal Dissociated Glucocorticoid Agonists Containing Azaindoles as Steroid A-Ring Mimetics

Doris Riether,\* Christian Harcken, Hossein Razavi, Daniel Kuzmich, Thomas Gilmore, Jörg Bentzien, Edward J. Pack, Jr., Donald Souza, Richard M. Nelson, Alison Kukulka, Tazmeen N. Fadra, Ljiljana Zuvela-Jelaska, Josephine Pelletier, Roger Dinallo, Mark Panzenbeck, Carol Torcellini, Gerald H. Nabozny, and David S. Thomson

*Department of Medicinal Chemistry, Department of Immunology and Inflammation, and Drug Discovery Support, Boehringer-Ingelheim Pharmaceuticals Inc., 900 Ridgebury Road, Ridgefield, Connecticut 06877*

Received June 21, 2010

Syntheses and structure–activity relationships (SAR) of nonsteroidal glucocorticoid receptor (GR) agonists are described. These compounds contain azaindole moieties as A-ring mimetics and display various degrees of in vitro dissociation between gene transrepression and transactivation. Collagen induced arthritis studies in mouse have demonstrated that in vitro dissociated compounds (**R**)-**16** and (**R**)-**37** have steroid-like anti-inflammatory properties with improved metabolic side effect profiles, such as a reduced increase in body fat and serum insulin levels, compared to steroids.

### Introduction

Glucocorticoid receptor agonists such as dexamethasone, prednisolone (Figure 1) and fluticasone esters have potent anti-inflammatory and immunosuppressive properties and are used for treating a variety of conditions including asthma<sup>1</sup> and rheumatoid arthritis.<sup>2</sup> However, steroid therapy is associated with characteristic side effects such as glucose intolerance, muscle wasting, skin thinning, and osteoporosis, which are the undesired outcomes of activating the glucocorticoid receptor (GR<sup>α</sup>).<sup>3</sup> In addition, cross-reactivity of steroids with the progesterone receptor (PR), androgen receptor (AR), and mineralocorticoid receptor (MR) can provoke off-target pharmacology.<sup>4</sup> The likelihood of identifying glucocorticoids (GC) with better safety profiles compared to existing therapies has increased significantly with newer understanding of the molecular mechanism of action.<sup>5</sup> While there is consensus that the desired anti-inflammatory effects of GC are mainly mediated via transrepression (TR), the repression of gene transcription<sup>6</sup> and the underlying molecular mechanisms for GC-mediated side effects are complex and only partially understood. However, recent data suggest that at least certain side effects are predominantly mediated via transactivation (TA) pathways.<sup>3,7</sup> After an agonist enters a target cell and binds to the GR, the ligand activated complex (GRC) translocates into the nucleus where direct and indirect functional pathways can be accessed. Acting directly, the GRC serves as an endogenous transcription factor by binding to specific DNA sequences and coactivator proteins, thereby initiating

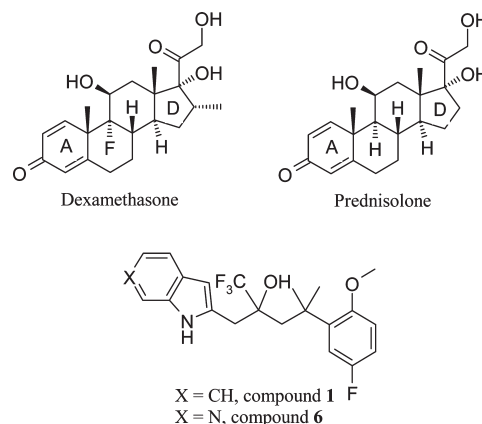


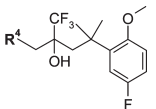
**Figure 1.** Synthetic glucocorticoid agonists.

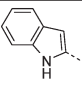
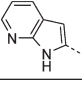
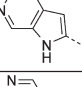
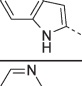
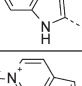
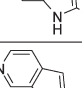
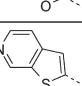
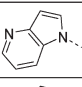
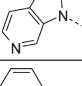
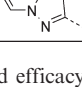
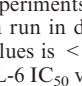
transcription of metabolic and endocrine genes. GRC-mediated transactivation of these genes is believed to contribute to the side effect profile of GC therapy.<sup>5</sup> Acting indirectly, the GRC adopts a conformation with an affinity for transcription factors (e.g., NF- $\kappa$ B and AP-1). Subsequent binding to these transcription factors results in the inhibition of expression of proinflammatory cytokines such as TNF- $\alpha$  and IL-6. This process, known as transrepression, is thought to contribute, in part, to the anti-inflammatory component of GC. Descriptions of the molecular basis for these pathways have been reported.<sup>3–7</sup> The differential molecular regulation of GC anti-inflammatory actions and their side effects is the basis for drug-discovery programs that are aimed at the development of dissociated GR ligands. These ligands would preferentially induce GR-mediated TR but demonstrate reduced or no TA. Recent publications describe nonsteroidal compounds that are selective and dissociated GR agonists.<sup>8</sup>

In our optimization effort to identify selective and dissociated nonsteroidal GR agonists, we started from compound **1**, which we previously described<sup>9</sup> and was a potent GR

\*To whom correspondence should be addressed. Phone: 1-203-791-6203. Fax: 1-203-791-6072. E-mail: doris.riether@boehringer-ingelheim.com.

<sup>a</sup>Abbreviations: GR, glucocorticoid receptor; PR, progesterone receptor; AR, androgen receptor; MR, mineralocorticoid receptor; GC, glucocorticoid; TR, transrepression; TA, transactivation; GRC, glucocorticoid receptor ligand activated complex; GR-LBD, glucocorticoid receptor ligand binding domain; HFF, human foreskin fibroblast; CIA, collagen induced arthritis; MMTV, mouse mammary tumor virus; LPS, lipopolysaccharide; TNF- $\alpha$ , tumor necrosis factor  $\alpha$ .

**Table 1.** In Vitro Biological Profile of A-Ring Mimetics<sup>a</sup>


	R <sup>4</sup>	GR IC <sub>50</sub> [nM]	PR IC <sub>50</sub> [nM]	MR IC <sub>50</sub> [nM]	IL-6 IC <sub>50</sub> [nM] (efficacy)
Dexamethasone	(Figure 1)	3.4	>2,000	33	0.51 (100%)
Prednisolone	(Figure 1)	15	>2,000	44	6.6 (91%)
1		21	250	380	6.6 (87%)
5		21	>2000	910	>2000 (23%)
6		4.4	>2000	580	9.8 (92%)
7		7.3	>2000	320	8.2 (95%)
8		23	>2000	>2000	120 (43%)
9		860	>2000	>2000	nd
11		22	>2000	1050	>2000 (19%)
12		7.1	1300	220	35 (66%)
13		2.0	200	48	2.8 (90%)
14		1400	>2000	>2000	nd
15		690	>2000	>2000	>2000 (-4%)

<sup>a</sup> IC<sub>50</sub> and efficacy values were determined from at least two independent experiments, using 11-point concentration dose-response curves, each run in duplicate. The standard deviation of the mean of GR IC<sub>50</sub> values is < 50%; PR IC<sub>50</sub> values is < 76%; MR IC<sub>50</sub> values is < 34%; IL-6 IC<sub>50</sub> values is < 62%; IL-6 efficacy is < 38%. nd = not determined.

agonist with only moderate selectivity against PR and MR (Table 1). Thus, our research initially focused on the nuclear receptor selectivity of **1**. Steroid A-ring mimetics that we<sup>10</sup> and others<sup>11</sup> described have demonstrated that both the A-ring and D-ring portion play an important role for binding affinity and nuclear receptor selectivity. On the basis of a docking study with GLIDE<sup>12</sup> using a model derived from a published X-ray crystal structure of GR with dexamethasone,<sup>13</sup> the indole moiety of compound **1** overlaid with the A-ring of the steroid in such fashion that the indole nitrogen formed a hydrogen bond with leucine 563. However, the hydrogen bond interaction of the dexamethasone carbonyl oxygen with glutamine 570 and arginine 611 was absent in **1** because of the lack of a potential hydrogen bond acceptor. Thus, we envi-

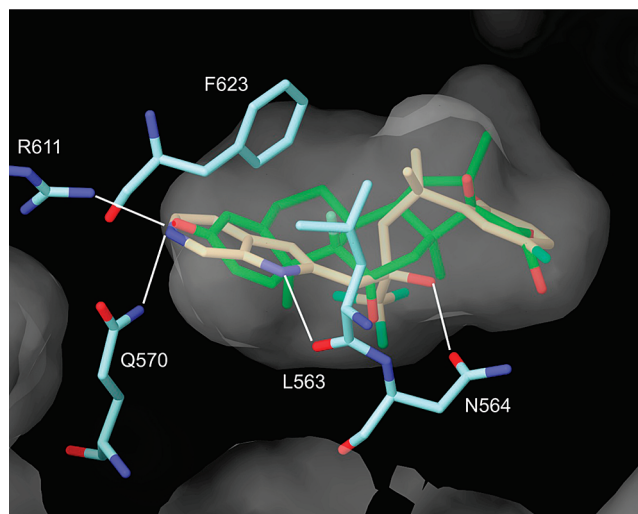


**Figure 2.** Docking results for dexamethasone (green) and **6** (cream) into the GR-LBD using the GR-LBD/dexamethasone co-complex X-ray structure.<sup>13</sup> Potential H-bonds with **6** are indicated by white lines.

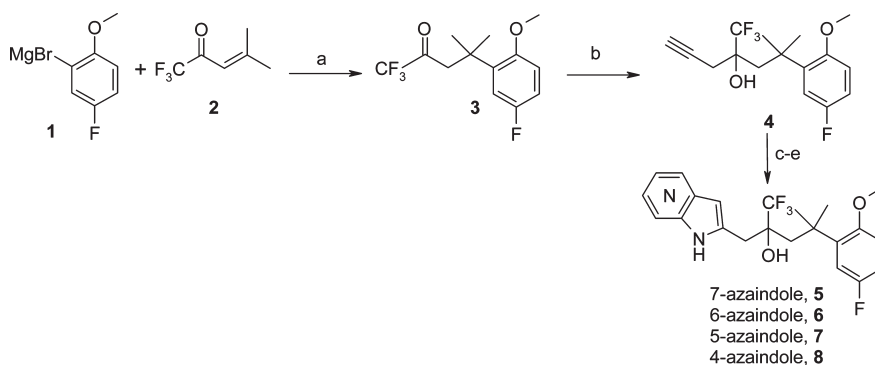
sioned replacing an indole carbon with nitrogen to better mimic the A-ring of the steroid (compounds **5–8**, Scheme 1). Because of similarities between the A-ring pockets of GR, MR, and PR (e.g., the glutamine and arginine pair is conserved in all three structures), it was not immediately clear how the introduction of an H-bond acceptor would impact the receptor selectivity. However, an effect on residues indirectly involved in binding may be hypothesized to effect selectivity (e.g., cysteine 622 in GR vs tyrosine 777 in PR and tyrosine 828 in MR). Various A-ring mimetics reported previously<sup>8c</sup> demonstrated that the selectivity profile can be impacted with this portion of the molecule. On the basis of molecular modeling, the 5- and the 6-position of the indole appeared to be best suited for introducing the hydrogen bond acceptor, e.g., 6-azaindole **6** (Figure 2). Besides the effect on selectivity, we were interested in the dissociation profile of these novel A-ring mimetics.

In addition, we also examined how modifications on the phenyl portion of **6**, which based on molecular modeling resides adjacent to the steroid D-ring domain, affect receptor potency, selectivity, and dissociation. The anti-inflammatory properties and side effect profiles of selective and dissociated GR agonists were then assessed in vivo.

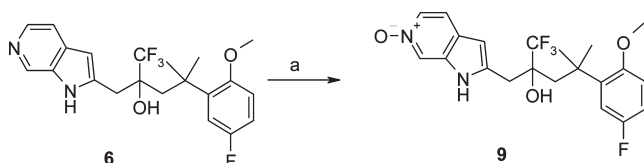
The syntheses and biological in vitro and in vivo profiles of azaindole compounds are the subject of this article.

## Chemistry

Aza-analogues **5–8** were synthesized according to Scheme 1. The preparation of trifluoro ketone **3** was accomplished via copper-mediated 1,4-addition of Grignard reagents **1** to 1,1,1-trifluorobut-3-en-2-one (**2**). Propargylation with propargylaluminum sesquibromide, which was prepared from aluminum amalgam and propargyl bromide, gave **4**. Sonogashira coupling of **4** with various halogen containing Boc-protected aminopyridines<sup>14</sup> followed by deprotection with hydrogen chloride in ethyl acetate and cyclization with KO<sup>t</sup>Bu in NMP afforded 7-, 6-, 5-, and 4-azaindole isomers **5–8**. Subsequently, compounds **6** and **7** were resolved by chiral HPLC to furnish the corresponding eutomers (**R**)-**6** and (**R**)-**7**.<sup>15</sup> Additionally, compound **6** was converted to the pyridine N-oxide **9** by treatment with mCPBA (Scheme 2).

Scheme 1. Synthesis of 7-, 6-, 5-, and 4-Azaindole Analogues<sup>a</sup>

<sup>a</sup> Reagents and conditions: (a) CuI (1.1 equiv), THF,  $-20^{\circ}\text{C}$ , 30 min, then **2** (1.1 equiv), room temperature, overnight, yield 46%; (b) Al,  $\text{HgCl}_2$ , THF, propargyl bromide,  $40^{\circ}\text{C}$ , 1 h, then **3**,  $-78^{\circ}\text{C}$ , 3 h, then room temperature, 9 h, yield 92%; (c) halogenopyridine (1 equiv), CuI (0.1 equiv), DMF,  $\text{NEt}_3$ ,  $\text{Pd}(\text{PPh}_3)_2\text{Cl}_2$  (0.05 equiv), room temperature, 15 h; (d) HCl, ethyl acetate, 5 h, room temperature; (e) NMP,  $\text{KOTu}$  (2.2 equiv), room temperature, 17 h, yield 5–57% over three steps.

Scheme 2. Synthesis of *N*-Oxide<sup>a</sup>

<sup>a</sup> Reagents and conditions: (a) MCPBA (1.5 equiv), DME, 2 h, yield 41%.

Scheme 3 outlines the syntheses of compounds **11**–**14**. For the synthesis of furo[2,3-*c*]pyridine **11** an inseparable mixture of 2-methylfuran[2,3-*c*]pyridine and 2-methylfuro[3,2-*b*]pyridine was deprotonated with lithium diisopropylamide (LDA) and added to trifluoro ketone **3**. The resultant isomers were then separated via column chromatography. Thieno[2,3-*c*]pyridine **12** was prepared from addition of the anion of thieno[2,3-*c*]pyridine to epoxide **10**, which was synthesized from trifluoro ketone **3** using dimethyloxosulfonium methylide derived from trimethylsulfoxonium iodide and sodium hydride. Furthermore, compounds **13** and **14** were accessed via the addition of the anion of 1*H*-pyrrolo[2,3-*c*]pyridine and 1*H*-pyrrolo[3,2-*b*]pyridine, respectively, to epoxide **10**.

Pyrazolo[1,5-*a*]pyridine **15** was synthesized by Sonogashira coupling of alkyne **4** and 2-iodopyridine, followed by the amination of the pyridine nitrogen of the resultant intermediate with ethyl-*O*-mesitylsulfonylacetohydroxamate and cyclization with  $\text{K}_2\text{CO}_3$  (Scheme 4).

The conversion of methoxy analogues (*R*)-**6** and (*R*)-**7** to the hydroxyl analogues (*R*)-**16** and (*R*)-**17** was accomplished with boron tribromide ( $\text{BBr}_3$ ) in dichloromethane (Scheme 5).

The same reaction sequence as outlined for compounds **6** and **7** (Scheme 1) was employed for the syntheses of 6-azaindole analogues **31**–**34** using alkynes **27**–**30** and Boc-protected 3-amino-4-iodopyridine as coupling partners (Scheme 6). In an effort to identify more efficient conditions for the synthesis and purification of azaindole compounds, we found that the cyclization and deprotection of the Sonogashira coupling product can be accomplished using DBU in methanol and water.<sup>16</sup> This method was used for the preparation of compound **34**.

Suzuki coupling of **34** with phenylboronic acid using  $\text{Pd}(\text{OAc})_2$  as a catalyst, (2-dicyclohexylsophino)biphenyl as a ligand, and KF as a base gave **35** (Scheme 7). The 4-pyridyl analogue **36** and 3,5-pyrimidinyl analogue **37** were

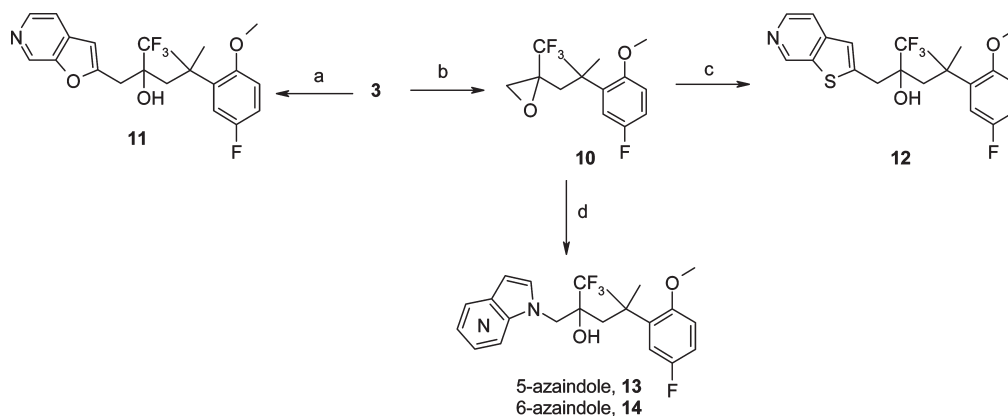
also prepared from **34** and their corresponding boronic acids, using  $\text{Pd}(\text{PPh}_3)_4$  as catalyst and  $\text{K}_2\text{CO}_3$  as a base. Demethylation of **35** and **36** to yield the hydroxyl analogues **38** and **39** was accomplished using  $\text{BBr}_3$ . Under the same demethylation conditions, no reaction was observed with the pyrimidine analogue **37**. However, the hydroxypyrimidinyl analogue **41** could be prepared by Suzuki coupling using hydroxylbromo compound **40**,  $\text{Pd}(\text{PPh}_3)_4$  as a catalyst, and  $\text{K}_2\text{CO}_3$  as a base.

Dihydrobenzofuran analogues **55**–**57** were prepared according to the sequence illustrated in Scheme 8. Addition of methylallylmagnesium chloride (**43**) to trifluoropyruvate (**42**) afforded the hydroxyl ester **44**, which upon Friedel–Crafts alkylation with unsubstituted or fluorinated dihydrobenzofuran and aluminum trichloride gave esters **45** and **46**. Alternatively, the chlorobenzofuran analogue **47** was prepared via chlorination of **45**. Reduction of **45**–**47** followed by periodate cleavage of the resultant diols provided trifluoro ketones **48**–**50**. Propargylation and Songashira coupling led to **53** and **54**, which upon deprotection and cyclization gave **55** and **57**. The fluorodihydrobenzofuran compound **56** was prepared by a more concise albeit lower yielding synthesis, in which the dianion of 2-methyl-1*H*-pyrrolo[2,3-*c*]pyridine was condensed with trifluoromethyl ketone **49**.

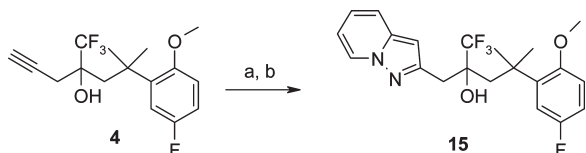
## Results and Discussion

Binding affinities for nuclear receptors were determined using a competition binding assay in which tetramethylrhodamine-labeled dexamethasone was used as a fluorescent probe for GR and MR and tetramethylrhodamine-labeled mifepristone was used for PR. Anti-inflammatory activities of test compounds (i.e., transrepression activity) were measured by IL-1 induced IL-6 production in human foreskin fibroblast (HFF) cells, and the efficacies were reported as a percentage of repression observed with dexamethasone.<sup>17</sup> Transactivation of compounds was determined by the ability to activate the MMTV promoter in HeLa cells transfected with an MMTV luciferase construct. As a second counterscreen for transactivation, compounds were tested for their abilities to induce aromatase in HFF cells. Comparison with dexamethasone established the basis for identifying compounds with a dissociated profile.

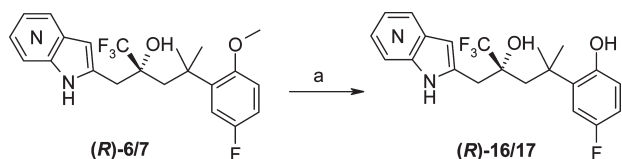
The effects of introducing a nitrogen into the indole portion of compound **1** are demonstrated in Table 1. Positioning the hydrogen bond acceptor in the 7- and 4-position of the indole, as in compounds **5** and **8**, respectively, had no impact on the

**Scheme 3.** Synthesis of Furanopyridine, Thienopyridine, and 1-Substituted Azaindole<sup>a</sup>

<sup>a</sup> Reagents and conditions: (a) 2-methylfuro[2,3-*c*]pyridine (1.5 equiv), THF, LDA (3 equiv),  $-78^{\circ}\text{C}$ , then **3**, yield 18%; (b) trimethylsulfoxonium iodide (1.2 equiv), DMSO, NaH (1.2 equiv), 30 min, then **3** in DMSO; (c) thieno[2,3-*c*]pyridine (1.3 equiv), <sup>t</sup>BuLi (1.3 equiv), THF,  $-78^{\circ}\text{C}$ , 20 min, then **10**, room temperature, overnight, yield 11% over two steps; (d) 1*H*-pyrrolo[2,3-*c*]pyridine (1.3 equiv), DMF, NaH (1.4 equiv), 30 min, then **10**, yield 6–30%.

**Scheme 4.** Synthesis of Pyrazolopyridine<sup>a</sup>

<sup>a</sup> Reagents and conditions: (a) 2-iodopyridine (1 equiv), CuI (0.1 equiv), DMF, NEt<sub>3</sub>, Pd(PPh<sub>3</sub>)<sub>2</sub>Cl<sub>2</sub> (0.05 equiv), room temperature, 15 h; (b) ethyl *O*-mesitylsulfonylacetohydroxamate (1.6 equiv), dioxane, perchloric acid (3.5 equiv),  $0^{\circ}\text{C}$ , 30 min, then room temperature, 4 days, yield 7% over two steps.

**Scheme 5.** Synthesis of Desmethyl Compounds<sup>a</sup>

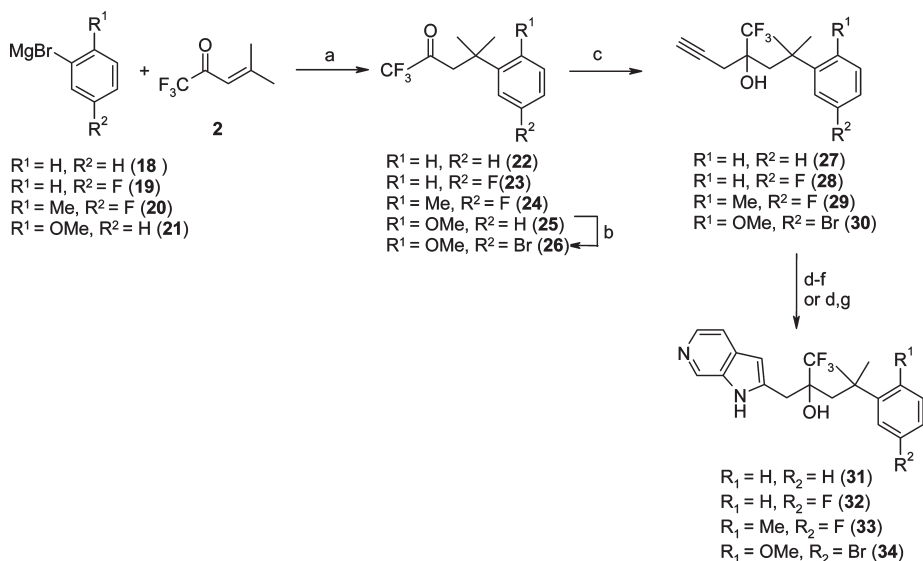
<sup>a</sup> Reagents and conditions: (a) BBr<sub>3</sub> (1 equiv), DCM,  $0^{\circ}\text{C}$ , 4–24 h, yield 64–80%.

GR binding affinity, while a 4-fold improvement was observed for compounds **6** and **7**, which was consistent with our hypothesis based on the modeling studies. Improvements in GR vs PR and MR selectivity were observed with all aza-analogues **5**–**8**. 6-Azaindole **6** displayed a very attractive potency/selectivity profile with a GR IC<sub>50</sub> value of 4.4 nM and selectivity against PR and MR of > 100 fold. 6- and 5-azaindole compounds **6** and **7** retained their ability to inhibit IL-1-stimulated IL-6 release in HFF cells with IC<sub>50</sub> values of 9.8 and 8.2 nM, respectively, and exhibited full efficacy compared to dexamethasone. The 7- and 4-azaindoles **5** and **8** also appeared to interact favorably with the GR-LBD as demonstrated by their binding affinities. However, the resulting ligand-bound receptors demonstrated a loss of activity in the IL-6 assay and thus was hypothesized to adopt conformations that were incapable of interacting effectively with anti-inflammatory transcription factors.<sup>18</sup> Oxidizing the aza-analogue **6** to the corresponding *N*-oxide **9** had a detrimental effect on the binding affinity. The role of the indole nitrogen was assessed by its replacement with oxygen (compound **11**) and sulfur (compound **12**). In both cases, the replacement of

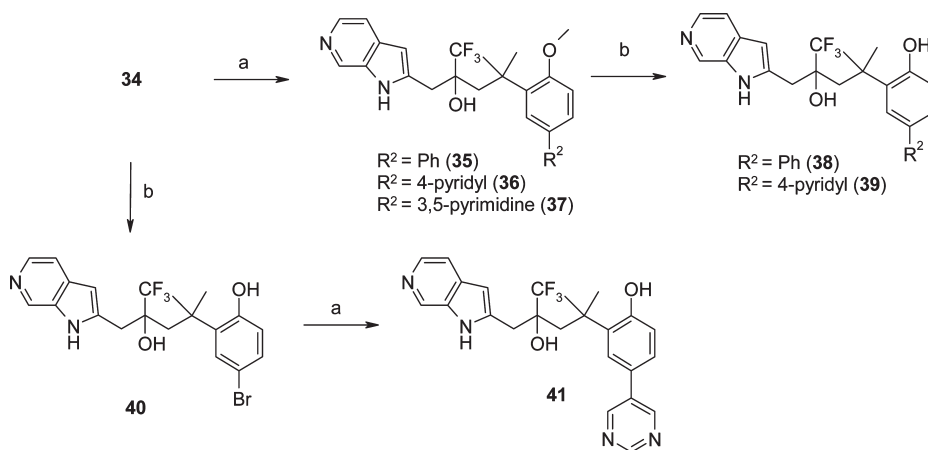
the nitrogen had minor effects on binding affinities when compared to **6**. Although the transrepression ability of furanopyridine **11** as measured by IL-6 potency and efficacy was completely abolished, it was only diminished 5-fold for thienopyridine **12** with a considerable reduction in efficacy. These data suggested a crucial role for the indole nitrogen, which was proposed to interact via a hydrogen bonding interaction with leucine 563 by our modeling studies. The data for the N-linked 4-azaindole compound **13**, which demonstrated a binding affinity for GR of 2.0 nM and an IC<sub>50</sub> value of 2.8 nM in the IL-6 assay, did however suggest that the hydrogen bonding interaction with leucine 563 was not essential.

Interestingly, selectivity over PR and MR was decreased for compound **13** relative to the C-2 linked azaindoles. Compounds **14** and **15** further supported our understanding of the H-bond requirements, as they demonstrated a dramatic loss in GR binding affinity, and were not expected to efficiently undergo any of the essential hydrogen bond interactions required for both affinity to the receptor as well as agonist activity. By changing the H-bonding capabilities, there is likely also a steric component that leads to the loss in GR potency. The loss of binding affinity in **14** seems to be more than compensated by moving the nitrogen from the 6- to the 4-position in compound **13**. Our hypothesis is that the pyridine nitrogen in **13** is acting as a H-bond acceptor to Q570/R611. Compound **14** does not have this capability.

With the goal to further assess azaindole compounds **6** and **7**, the racemic compound **6** was resolved by chiral HPLC and (*R*)-**7** was made from (*R*)-**4**, which is derived from an intermediate for which the absolute configuration had been determined by X-ray crystallographic analysis.<sup>15</sup> The data for the enantiomers (*R*)-**6**, (*S*)-**6**, and (*R*)-**7** are shown in Table 2; the difference in binding affinity between (*R*)-**6** and (*S*)-**6** is consistent with the importance of the H-bond between the hydroxyl group and asparagine 564, as was predicted by our modeling studies. As expected, both enantiomers demonstrated improved binding affinity and cellular potency compared to the racemic mixtures. Compounds (*R*)-**6** and (*R*)-**7** fulfilled our primary objective of improving the nuclear receptor selectivity profile of compound **1**. In our effort to identify GR agonists that could distinguish between transrepression and transactivation pathways (i.e., are dissociated), compounds (*R*)-**6** and (*R*)-**7** were tested for their ability to activate

Scheme 6. Synthesis of 6-Azaindole Compounds<sup>a</sup>

<sup>a</sup> Reagents and conditions: (a) CuI (1.1 equiv), THF,  $-20\text{ }^\circ\text{C}$ , 30 min, then **2** (1.1 equiv), room temperature, overnight, yield 42–84%; (b) NBS (1.1 equiv),  $\text{CCl}_4$ , reflux, 20 h, yield 94–99%; (c) Al,  $\text{HgCl}_2$ , THF, propargyl bromide,  $40\text{ }^\circ\text{C}$ , 1 h, then ketones **22–24**, or **26**,  $-78\text{ }^\circ\text{C}$ , 3 h, then room temperature, 9 h, yield 73%; (d) (4-iodopyridin-3-yl)carbamic acid *tert*-butyl ester (1 equiv), CuI (0.1 equiv), DMF,  $\text{NEt}_3$ ,  $\text{Pd}(\text{PPh}_3)_2\text{Cl}_2$  (0.05 equiv), room temperature, 15 h; (e) HCl, ethyl acetate, 5 h, room temperature; (f) NMP,  $\text{KO}^t\text{Bu}$  (2.2 equiv), room temperature, 17 h; (g) DBU, MeOH, water,  $65\text{ }^\circ\text{C}$ , yield 14–54% over three steps (d–f) or two steps (d, g).

Scheme 7. Synthesis of Biaryl Compounds<sup>a</sup>

<sup>a</sup> Reagents and conditions: (a) boronic acid (1.5 equiv), Pd-catalyst/ligand, DMF, MeOH, DME,  $80\text{ }^\circ\text{C}$ , 12 h, yield 2–45%; (b)  $\text{BBr}_3$  (1 equiv), DCM,  $0\text{ }^\circ\text{C}$ , 4–24 h, yield 29–87%.

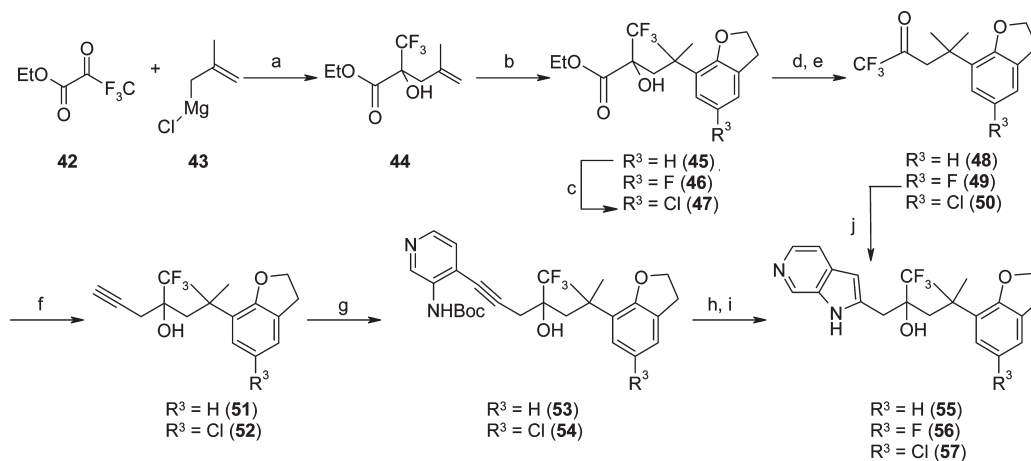
MMTV and induce aromatase expression. A compound can be characterized as dissociated *in vitro* if it displays weak activity, low efficacy, or both in the transactivation compared to the transrepression assay. Therefore, both compounds (**R**-6 and **R**-7) were classified as dissociated in the MMTV assay, since they were weak partial agonists demonstrating low efficacy. In the aromatase induction assay (**R**-7) was relatively potent and efficacious compared to dexamethasone ( $\text{IC}_{50} = 7\text{ nM}$ , 78% efficacy); thus, it was not deemed as dissociated. When testing (**R**-6) in the aromatase induction assay, an initial increase followed by a drop in estradiol levels was obtained leading to the hypothesis that (**R**-6) not only induces aromatase but also acts as its inhibitor. Upon testing in an aromatase inhibition assay, an  $\text{IC}_{50}$  of  $1.1\text{ }\mu\text{M}$  was determined. Thus, the data from the aromatase induction assay could not be accurately interpreted for (**R**-6).

Pharmacokinetic studies of (**R**-6) in Sprague–Dawley rats demonstrated a high clearance and a moderately high volume

of distribution resulting in a moderate half-life and low bioavailability (Table 3). Since demethylation of the methoxy group was considered a potential metabolic liability, the plasma levels of des-methyl compound (**R**-16) were also measured upon oral administration of (**R**-6). The results indicated large  $C_{\text{max}}$  levels and AUC values for both the parent (**R**-6) and the des-methyl metabolite (**R**-16).

On the basis of this finding, des-methyl metabolites (**R**-16 and **R**-17) were synthesized and evaluated in our *in vitro* assays. They proved to be equipotent to their respective parent compounds (i.e., (**R**-6 and **R**-7) while retaining a similar dissociation profile with 30% and 45% efficacy in the MMTV assay, respectively. However, both compounds showed a lack of dissociation in the aromatase induction assay (Table 4).

We then examined the effect of varying the substitution on the phenyl portion of the molecule, which based on molecular modeling in the GR-LBD overlaid with the steroid's D-ring. Effects of various phenyl substituents on binding and cellular

Scheme 8. Synthesis of Dihydrobenzofurans<sup>a</sup>

<sup>a</sup> Reagents and conditions: (a) THF,  $-65^{\circ}\text{C}$ , then methylallylmagnesium chloride (1.3 equiv), 4 h, room temperature, 12 h, yield 61%; (b) dihydrobenzofurane (1.1 equiv), dichloroethane,  $\text{AlCl}_3$  at  $0^{\circ}\text{C}$ , then room temperature, 12 h, yield 30–31%; (c) acetic acid,  $15^{\circ}\text{C}$ ,  $\text{Cl}_2$ ; (d)  $\text{LiAlH}_4$ , THF, 48 h; (e)  $\text{NaIO}_4$ , MeOH, 12 h, yield 24–98% over two/three steps; (f) Al,  $\text{HgCl}_2$ , THF, propargyl bromide,  $40^{\circ}\text{C}$ , 1 h, then **48** or **50**,  $-78^{\circ}\text{C}$ , 3 h, room temperature, 9 h, yield 64–95%; (g) halogeno pyridine (1 equiv), CuI (0.1 equiv), DMF,  $\text{NEt}_3$ ,  $\text{Pd}(\text{PPh}_3)_2\text{Cl}_2$  (0.05 equiv), room temperature, 15 h, yield 64–73%; (h) HCl, ethyl acetate, 5 h, room temperature; (i) NMP,  $\text{KO}^t\text{Bu}$  (2.2 equiv), room temperature, 17 h, yield 30–31% over two steps; (j) pyrrolopyridine, *n*-BuLi (3 equiv), THF,  $-78^{\circ}\text{C}$ , 5 min,  $\text{KO}^t\text{Bu}$  (2 equiv), room temperature, 1 h, then **49** at  $-78^{\circ}\text{C}$ , yield 7%.

Table 2. In Vitro Biological Profiles of *R*-Enantiomers (**R**-6 and **7**)<sup>a</sup>

		GR IC <sub>50</sub> [nM]	PR IC <sub>50</sub> [nM]	MR IC <sub>50</sub> [nM]	IL-6 IC <sub>50</sub> [nM] (efficacy)	MMTV IC <sub>50</sub> [nM] (efficacy)	Aromatase EC <sub>50</sub> [nM] (efficacy)
<b>(R)</b> -6		1.4	1150	380	6.0 (93%)	20 (10%)	nd
<b>(S)</b> -6		1700	>2000	>2000	430 (86%)	nd	nd
<b>(R)</b> -7		1.4	600	58	2.0 (93%)	22 (35%)	6.8 (78%)

<sup>a</sup> IC<sub>50</sub> and efficacy values were determined from at least two independent experiments, using 11-point concentration dose-response curves, each run in duplicate except for MMTV values, which used 8-point instead of 11-point concentration curves. The standard deviation of the mean of GR IC<sub>50</sub> values is < 116%; PR IC<sub>50</sub> values is < 37%; MR IC<sub>50</sub> values is < 31%; IL-6 IC<sub>50</sub> values is < 11%; IL-6 efficacy is < 2%; MMTV IC<sub>50</sub> values is < 25%; aromatase IC<sub>50</sub> values is < 38%; aromatase efficacy is < 12%. nd = not determined.

activity are summarized in Table 5. Removing the methoxy group and fluorine atom from **6** (i.e., compound **31**) resulted in decreased selectivity against PR, a ~3-fold loss in IL-6 potency and lower transrepression efficacy. A similar profile was obtained by only removing the methoxy group from **6** (i.e., compound **32**), although in this case, the loss in IL-6 potency was slightly more pronounced (10-fold). Both compounds **31** and **32** also were less potent and less efficacious in the transactivation assays compared to **(R)**-16 and **17**. With the exception of the PR selectivity, replacing the methoxy group of **6** with a methyl group led to a profile that was

Table 3. Sprague–Dawley Rat Pharmacokinetics of (**R**-6)<sup>a</sup>

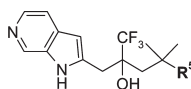
	<b>(R)</b> -6	<b>(R)</b> -16
CL (iv) [(mL/min)/kg]	61	nd
<i>V</i> <sub>SS</sub> (iv) [L/kg]	8.7	nd
<i>t</i> <sub>1/2</sub> (iv) [h]	1.7	nd
<i>C</i> <sub>max</sub> (po) [ng/mL] ( <i>t</i> <sub>max</sub> )	427 (2 h)	444
AUC <sub>inf</sub> (po) [h·ng/mL]	1740	2236
<i>F</i> (po) [%]	21	nd

<sup>a</sup> Dosed at 5 mg/kg iv in a PEG400/water (80:20) vehicle and at 30 mg/kg po as a suspension in 1% aqueous methylcellulose, mean of three rats. nd = not determined.

**Table 4.** In Vitro Biological Profiles of Des-methyl Metabolites (**R**)-16 and (**R**)-17<sup>a</sup>

		GR IC <sub>50</sub> [nM]	PR IC <sub>50</sub> [nM]	MR IC <sub>50</sub> [nM]	IL-6 IC <sub>50</sub> [nM] (efficacy)	MMTV IC <sub>50</sub> [nM] (efficacy)	Aromatase EC <sub>50</sub> [nM] (efficacy)
<b>(R)</b> -16		2.1	1200	210	3.3 (93%)	80 (30%)	11 (84%)
<b>(R)</b> -17		4.7	1900	220	3.0 (94%)	56 (45%)	11 (149%)

<sup>a</sup> IC<sub>50</sub> and efficacy values were determined from at least two independent experiments, using 11-point concentration dose-response curves, each run in duplicate except for MMTV values, which used 8-point instead of 11-point concentration curves. The standard deviation of the mean of GR IC<sub>50</sub> values is < 62%; PR IC<sub>50</sub> values is < 62%; MR IC<sub>50</sub> values is < 70%; IL-6 IC<sub>50</sub> values is < 83%; IL-6 efficacy is < 1%; MMTV IC<sub>50</sub> values is < 36%; aromatase IC<sub>50</sub> values is < 58%; aromatase efficacy is < 15%.

**Table 5.** In Vitro Biological Profiles of Various R<sup>5</sup> Modifications<sup>a</sup>

	R <sup>5</sup>	GR IC <sub>50</sub> [nM]	PR IC <sub>50</sub> [nM]	MR IC <sub>50</sub> [nM]	IL-6 IC <sub>50</sub> [nM] (efficacy)	MMTV IC <sub>50</sub> [nM] (efficacy)	Aromatase EC <sub>50</sub> [nM] (efficacy)		R <sup>5</sup>	GR IC <sub>50</sub> [nM]	PR IC <sub>50</sub> [nM]	MR IC <sub>50</sub> [nM]	IL-6 IC <sub>50</sub> [nM] (efficacy)	MMTV IC <sub>50</sub> [nM] (efficacy)	Aromatase EC <sub>50</sub> [nM] (efficacy)
<b>31</b>		9.3	190	810	31 (75%)	>2000 (6%)	>2000 (23%)		<b>38</b>	11	1300	160	15 (88%)	47 (45%)	40 (71%)
<b>32</b>		23	8	>2000	99 (73%)	nd	>2000 (26%)		<b>39</b>	6.6	>2000	230	23 (85%)	>2000 (30%)	nd# (9%)
<b>33</b>		10	1900	590	38 (89%)	nd	nd# (70%)		<b>41</b>	19	>2000	1700	21 (86%)	nd	nd
<b>35</b>		12	1200	480	40 (81%)	nd	69 (50%)		<b>55</b>	4.5	130	780	15 (88%)	>2000 (15%)	30 (24%)
<b>36</b>		8	>2000	390	30 (78%)	nd	>2000 (4%)		<b>56</b>	2.3	450	280	9.3 (91%)	>2000 (17%)	nd# (15%)
<b>37</b> <b>(R)</b> -37		27	>2000	>2000	50 (81%)	nd	nd# (6%)		<b>57</b>	7	1210	540	17 (93%)	>2000 (18%)	120 (86%)
		8.0	>2000	>2000	20 (78%)	>2000 (9%)	>2000 (6%)								

<sup>a</sup> IC<sub>50</sub> and efficacy values were determined from at least two independent experiments, using 11-point concentration dose-response curves, each run in duplicate except for MMTV values, which used 8-point instead of 11-point concentration curves. The standard deviation of the mean of GR IC<sub>50</sub> values is < 39%; PR IC<sub>50</sub> values is < 37%; MR IC<sub>50</sub> values is < 12%; IL-6 IC<sub>50</sub> values is < 18%; IL-6 efficacy is < 4%; MMTV IC<sub>50</sub> values is < 31%; aromatase IC<sub>50</sub> values is < 30%; aromatase efficacy is < 74%. nd = not determined. (#) Due to very low efficacy or no dose response curve based on aromatase inhibition.

comparable to that of the unsubstituted phenyl (compound **33** vs **31**). Although the original X-ray structure of dexamethasone bound to GR-LBD<sup>13</sup> suggested that large substituents in the

5-position of the phenyl were not tolerated (i.e., based on the size of the binding pocket), more recent X-ray structures showed that the GR-LBD could expand to accommodate

larger ligands. In particular the size of the D-ring pocket is expanded relative to that observed in the dexamethasone structure.<sup>19</sup> Thus, we explored larger substituents in the 5-position of the phenyl group, which is suggested by modeling to occupy the space of the D-ring in dexamethasone, to assess their effects on the binding and cellular profiles. The 2-methoxy and 2-hydroxy analogues of the 5-phenyl-, 5-pyridyl-, and 5-pyrimidylphenyl compounds **35–39** and **41** were synthesized. The overall observed trend was that the hydroxyl compounds **38**, **39**, and **41** were more potent and efficacious in inhibiting IL-1-induced IL-6 production than **35–37**. Compounds **36**, **37**, and **39** had an attractive overall profile; in particular, they were dissociated in the aromatase assay.<sup>20</sup> In order to establish a correlation between the binding interactions of these larger groups in the D-ring region and the TR/TA selectivity, further investigation is needed.

Since demethylation of the methoxy group had been observed in vivo with **6** and **7**, the plasma samples after oral administration of **35–37** to mice were analyzed to determine the exposure of the corresponding hydroxyl compounds (i.e., **38**, **39**, and **41**). In contrast to the 5-phenyl and the 5-fluoro analogues (i.e., **35** and **6**), the methoxy groups of 5-pyridyl compound **36** and 5-pyrimidyl compound **37** were not metabolically labile. Other explored R<sup>5</sup> groups included the unsubstituted dihydrobenzofuran **55** and halogenated dihydrobenzofurans **56** and **57**, which were comparable to **6** in GR binding and IL-6 potencies. It is noteworthy that the affinity for PR decreased with the size of the substituent on the dihydrobenzofuran moiety. Compounds **55–57** distinguished themselves based on their transactivation profiles. While all three compounds were dissociated in the MMTV assay, only **55** and **56** were significantly dissociated in the aromatase assay.

**In Vivo Rat Pharmacokinetic Studies.** (**R**)-**16** and (**R**)-**37** were selected for pharmacokinetic studies in rats based on their overall in vitro profiles. They displayed moderate and high clearances, moderately high volumes of distribution, and moderate half-lives after intravenous administration and good bioavailabilities after oral dosing (Table 6).

**In Vivo Pharmacology Studies.** In order to assess the in vivo anti-inflammatory properties and dissociation profile of these compounds, thus determining whether the in vitro transactivation assays lead to an in vivo dissociated profile, compounds (**R**)-**16** and (**R**)-**37** were tested in acute and chronic pharmacology models. A mouse model of LPS-stimulated TNF- $\alpha$  production was employed in which (**R**)-**16** and (**R**)-**37** in Cremophor were administered orally 1 h prior to an LPS challenge, and plasma TNF- $\alpha$  levels were determined 1 h after challenge. (**R**)-**16** and (**R**)-**37** exhibited potent in vivo anti-inflammatory activities with ED<sub>50</sub> values of < 0.3 and < 1 mg/kg, respectively.

Both the anti-inflammatory activities and side effect profiles were assessed in the mouse model of collagen induced arthritis (CIA), a chronic model of inflammatory polyarthritis that shares many features with human rheumatoid arthritis. B10.RIII mice were immunized with porcine type II collagen and complete Freund's adjuvant and then monitored for signs of arthritis. Animals were enrolled into the study at the first signs of disease (paw/joint swelling) and treated daily with compound, prednisolone, or vehicle for a period of 5 weeks. The animals were monitored regularly, and arthritis severity was assessed through clinical scoring of all four paws based on a score of 1–3. The clinical score per paw was summed to give a maximal severity score of 16 for

**Table 6.** Sprague–Dawley Rat Pharmacokinetics of (**R**)-**16**<sup>a</sup> and (**R**)-**37**<sup>b</sup>

	( <b>R</b> )- <b>16</b>	( <b>R</b> )- <b>37</b>
CL (iv) [(mL/min)/kg]	49	83
V <sub>SS</sub> (iv) [L/kg]	7.6	6.6
t <sub>1/2</sub> (iv) [h]	1.85	1.0
C <sub>max</sub> (po) [ng/mL]	509	422
AUC <sub>inf</sub> (po) [h·ng/mL]	4879	5930
F (po) [%]	48	97

<sup>a</sup> Dosed at 5 mg/kg iv in a PEG400/water (80:20) vehicle and at 30 mg/kg po as a suspension in 1% aqueous methylcellulose, mean of three rats.

<sup>b</sup> Dosed at 2 mg/kg iv in a PEG400/water (70:30) vehicle and at 30 mg/kg po in a PEG400/H<sub>2</sub>O/Tween (80/18/2) vehicle, mean of three rats.

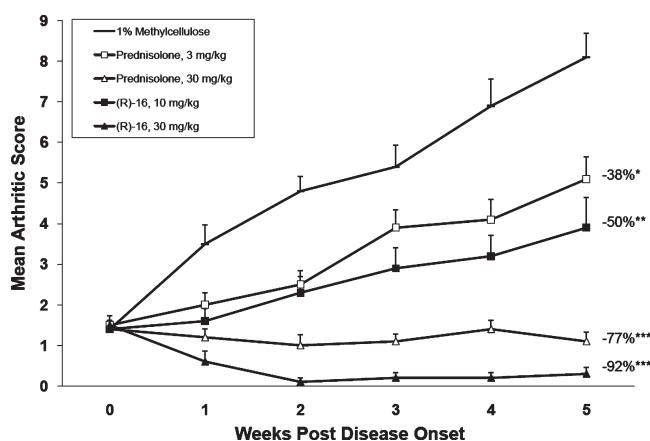


**Figure 3.** Collagen induced arthritis model: (**R**)-**16**. Data are given as the mean of 10 animals per group. Statistical analysis of AUCs was performed with the Mann–Whitney test: \*,  $p < 0.005$ , \*\*,  $p < 0.0005$ , \*\*\*,  $p < 0.0001$  compared to vehicle (1% aqueous methylcellulose).

each animal. (**R**)-**16** was evaluated in this model at once daily oral doses of 30 and 10 mg/kg for a period of 5 weeks versus prednisolone at 30 and 3 mg/kg. At the end of the study, serum was collected for biomarker analysis to assess the side effect profile. (**R**)-**16** significantly inhibited disease progression with the 30 mg/kg dose group exhibiting an improved efficacy (Mann–Whitney test:  $p = 0.0002$ ) of 92% compared to the 30 mg/kg prednisolone group (77%). On the basis of the efficacy obtained with the 10 mg/kg dose group, the ED<sub>50</sub> was determined to be 10 mg/kg (Figure 3).

To assess the in vivo dissociation profile, i.e., the metabolic side effect profile, body fat content, triglyceride, free fatty acid, and insulin levels were analyzed and compared between similarly efficacious doses of prednisolone (30 mg/kg) and (**R**)-**16** (30 mg/kg) (Figure 4). An increase in body fat content and serum insulin was obtained upon (**R**)-**16** treatment, which was however significantly lower compared to prednisolone treated animals. While prednisolone also induced a significant increase in triglycerides, animals treated with (**R**)-**16** showed no increase of triglyceride levels. In contrast, no significant difference was observed between the two compounds in regard to an increase in free fatty acids. We also assessed the side effect profiles of prednisolone and (**R**)-**16** in healthy (nonimmunized) animals (Figure 5) to avoid the complexity of the disease and its impacts on metabolic side effect biomarkers. After 5 weeks of dosing, prednisolone demonstrated a significant increase in body fat content, triglyceride, and serum insulin levels while (**R**)-**16** only showed a significant increase in triglyceride levels.



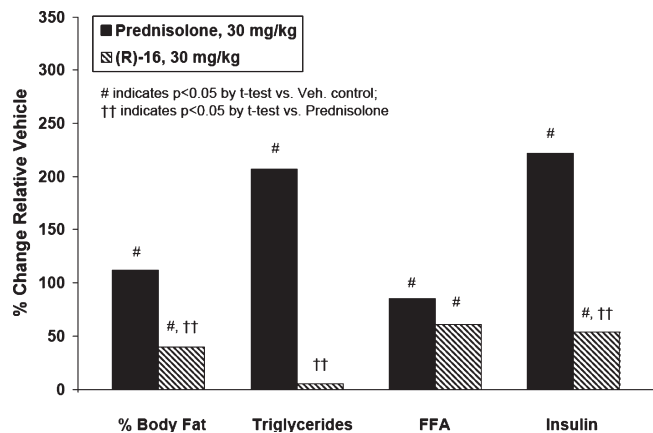


**Figure 4.** Side effect profile of (*R*)-16 and prednisolone in diseased mice.

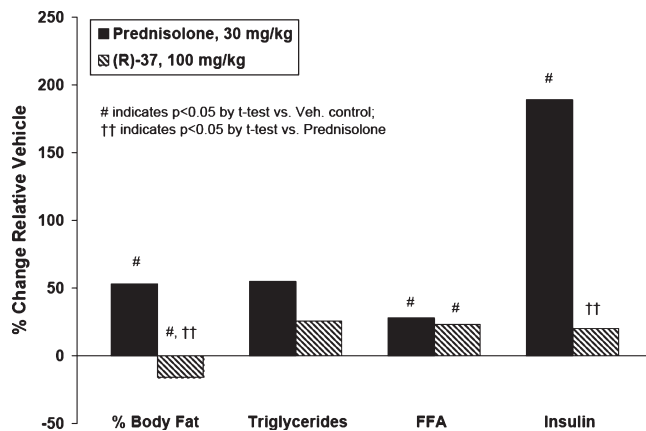


**Figure 7.** Side effect profile of prednisolone and (*R*)-37 in healthy mice.

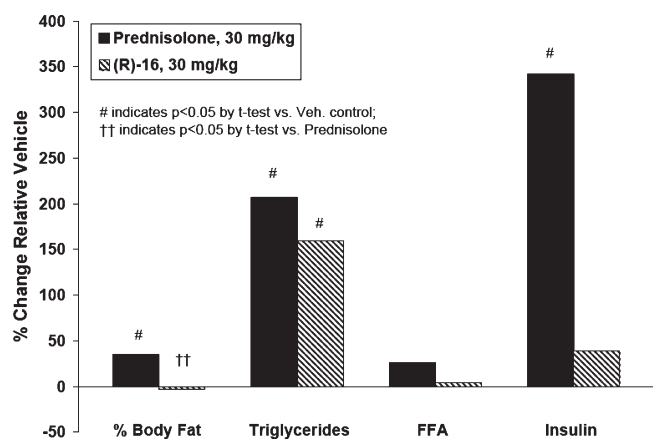


**Figure 5.** Side effect profile of prednisolone and (*R*)-16 in healthy mice.

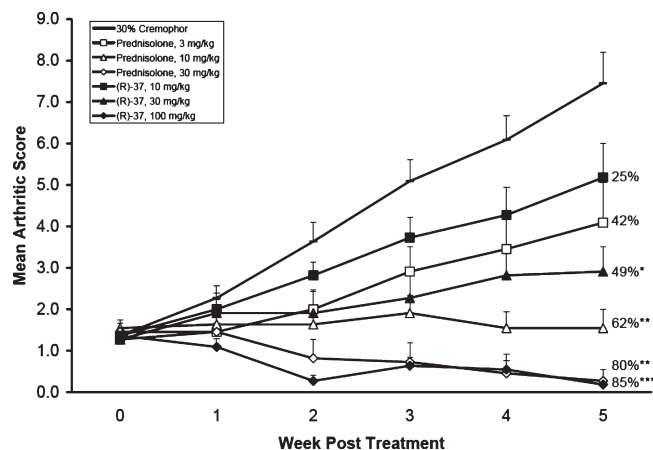


**Figure 6.** Collagen Induced arthritis model: (*R*)-37. Data are given as the mean of 10 animals per group. Statistical analysis of AUCs was performed with the Mann–Whitney test: \*,  $p < 0.001$ , \*\*,  $p < 0.0005$ , \*\*\*,  $p < 0.0001$  compared to vehicle (1% aqueous methylcellulose).

(*R*)-37 was tested in the mouse CIA model at 100, 30, and 10 mg/kg demonstrating an ED<sub>50</sub> of 30 mg/kg, while the 100 mg/kg group achieved similar efficacy to prednisolone at 30 mg/kg (Figure 6). Regarding the side effect profile of (*R*)-37 treated healthy animals, a clear difference was observed

for body fat content and serum insulin levels when compared to prednisolone treatment (Figure 7).

On the basis of these data, it can be concluded that the in vitro dissociation profiles of (*R*)-16 and (*R*)-37, in particular dissociation in the MMTV assay, clearly translated into improved metabolic side effect profiles in vivo compared to steroid treatment. Whether dissociation in the aromatase induction assay has an additional advantage compared to steroids remains unclear.

## Conclusion

5- and 6-azaindole A-ring mimetics with good binding affinity for GR and high selectivity against PR and MR were reported. Depending on the substitution pattern on the phenyl portion of the molecule, good transrepression activity in a cellular IL-6 assay with various degrees of transactivation activities in the MMTV or aromatase assays were achieved. Azaindoles (*R*)-16 and (*R*)-37 demonstrated good pharmacokinetic properties in rat. Additionally, (*R*)-16 and (*R*)-37 displayed potent inhibition of TNF- $\alpha$  production in a mouse proof of principle model of LPS challenge. Furthermore, they significantly inhibited disease progression in mouse collagen induced arthritis studies while achieving similar efficacy to prednisolone at equivalent anti-inflammatory doses. The in vitro dissociation profiles of (*R*)-16 and (*R*)-37 translated into improved in vivo metabolic side effect profiles compared to prednisolone. Thus, these compounds represent a generation of GR ligands with good clinical potential.

## Experimental Section

**Analytical Methods.** <sup>1</sup>H NMR spectra were recorded on a Bruker UltraShield 400 MHz spectrometer operating at 400 MHz in solvents, as noted. Proton coupling constants ( $J$  values) are rounded to the nearest 0.01 Hz. All solvents were HPLC grade or better. The reactions were followed by TLC on pre-coated Uniplate silica gel plates purchased from Analtech. The developed plates were visualized using 254 nm UV illumination or by PMA stain. Flash column chromatography on silica gel was performed on Redi Sep prepacked disposable silica gel columns using an Isco Combiflash or on traditional gravity columns. Reactions were carried out under an atmosphere of Ar at room temperature, unless otherwise noted. Mass spectrometry data were obtained using the Micromass Platform LCZ (flow injection). Purity was evaluated by the two methods described below and is  $\geq 95\%$  for all final compounds.

**System 1.** Analytical HPLC measurements were performed using a Varian Dynamax SD-200 pump coupled to a Varian Dynamax UV-1 detector. The solvents were the following: (A) water + 0.05% TFA; (B) acetonitrile + 0.05% TFA. Flow rate was 1.2 mL/min. The column was Vydac RP-18, 5 m, 250 mm  $\times$  4.6 mm. Photodiode array detector was set at 220 nm. The gradient was from 95% to 20% solvent A over 25 min.

**System 2.** LCMS experiments were performed with an HP 1110 Agilent using a quaternary G1311A pump coupled to a Micromass Platform LCZ detector. The solvents were the following: (A) water + 0.1% formic acid; (B) acetonitrile + 0.1% formic acid. Flow rate was 1.5 mL/min. Photodiode array detector was set at 190 or 400 nm for (a) Agilent Zorbax Eclipse XDB-C8 5  $\mu$ m, 4.6 mm  $\times$  150 mm column, 4.6 mm  $\times$  30 mm, 3.5  $\mu$ m, from 99% to 5% solvent A over 10 min or for (b) column Agilent Zorbax C18 SB 3.5  $\mu$ m, 4.6 mm  $\times$  30 mm cartridge, from 95% to 5% solvent A over 2.5 min.

**Chemistry. General Grignard Reaction Procedures To Afford Ketones 3, 22–25, 48, and 49.** To a 0–5 °C cold solution of **2** (158 mmol, 75% in ether/THF) and CuI (158 mmol) in ether (300 mL) is added the arylmagnesium halide (157 mmol). The mixture is warmed to room temperature, stirred overnight, and diluted with saturated aqueous NH<sub>4</sub>Cl (15 mL) and ethyl acetate. The organic layer is washed with water, brine and dried over MgSO<sub>4</sub>. Removal of the volatiles in vacuo provided a residue which is purified by flash silica gel chromatography using 0–5% ethyl acetate in hexanes as the eluent.

**General Propargylation Procedure To Afford Alkynes 4, 27, 28, 29, 30, 51, and 52.** Aluminum amalgam is prepared from aluminum foil (1.16 g, 14.4 mmol) and mercuric chloride (12 mg, catalytic amount) in anhydrous THF (20 mL) by vigorously stirring the mixture at room temperature for 1 h under an argon atmosphere. A solution of propargyl bromide (4.80 mL, 80 wt % in toluene, 43.1 mmol) in anhydrous THF (25 mL) is slowly added to a stirred suspension, maintaining a temperature of 30–40 °C, and stirring at 40 °C is continued until a dark gray solution is obtained (~1 h). The propargylaluminum sesquibromide solution is added to a solution of trifluoro ketone **3**, **22–25**, **48**, or **49** (14.4 mmol) in anhydrous ether (150 mL) at –78 °C. The reaction mixture is stirred at this temperature for 3 h and then is allowed to warm to room temperature, at which time it is stirred for 12 h. The reaction mixture is then poured into ice–water (20 mL) and extracted with ether (4  $\times$  30 mL). The combined extracts are washed with brine (20 mL), dried over MgSO<sub>4</sub>, and concentrated. The residual oil is subjected to flash silica gel chromatography using 5–15% ethyl acetate in hexanes.

**General Sonogashira Coupling Procedure.** To a solution of halogeno pyridine (1 mmol) in anhydrous DMF (1 mL) and NEt<sub>3</sub> (3 mL) are added CuI (0.10 mmol), Pd(PPh<sub>3</sub>)<sub>2</sub>Cl<sub>2</sub> (0.05 mmol), and the alkyne **4**, **27**, **28**, **29**, **30**, **51**, or **52** (1 mmol) under argon, and the mixture is stirred at room temperature for 15 h. The mixture is diluted with EtOAc (10 mL), washed with saturated aqueous NH<sub>4</sub>Cl solution (2  $\times$  5 mL), and the combined aqueous layers are extracted with EtOAc (3  $\times$  20 mL). The combined organic layers are washed with brine (5 mL), dried over MgSO<sub>4</sub>, and concentrated. Flash silica gel chromatography using 15–30% ethyl acetate in hexanes gives the coupling product as a white solid.

**General Boc-Deprotection Procedure.** Boc-protected amino pyridine (Sonogashira coupling product) (4 mmol) in a saturated solution of HCl in ethyl acetate (40 mL) is stirred at room temperature for 5 h. Then the solvent is removed in vacuo and the residual oil is diluted with ether (10 mL) and concentrated to give a solid, which is carried on to the next step without further purification.

**General Cyclization Procedure A.** To a solution of aminopyridine hydrochloride salt (Boc-deprotection product) (3.9 mmol) in anhydrous NMP (100 mL) is added KO<sup>t</sup>Bu (8.6 mmol), and the mixture is stirred under argon at room temperature for 17 h.

The reaction mixture is diluted with ether (30 mL) and washed with water (15 mL). The aqueous layer is extracted with ether (3  $\times$  20 mL), and the combined organic layers are washed with water (2  $\times$  5 mL) and brine (5 mL), dried over MgSO<sub>4</sub>, and concentrated. Flash silica gel chromatography using 0–10% MeOH in CH<sub>2</sub>Cl<sub>2</sub> gives the azaindole as a white solid.

**General Cyclization Procedure B.** To a solution of Boc protected aminopyridine (Sonogashira coupling product) (4 mmol) in MeOH (50 mL) and water (11 mL) is added DBU and the reaction mixture heated to 65 °C for 2 h. The reaction mixture is concentrated to 30 mL, and water (10 mL) is added. The azaindole product is precipitated, filtered, and dried.

**General Demethylation Procedure.** To a solution of the methoxy compound (1.65 mmol) in CH<sub>2</sub>Cl<sub>2</sub> (25 mL) is added BBr<sub>3</sub> (1.65 mmol, 1 M in CH<sub>2</sub>Cl<sub>2</sub>) under argon and at 0 °C. The reaction mixture is stirred for 4–24 h at 0 °C and then quenched with MeOH (10 mL). The solvents are evaporated, and the residue is dissolved in ethyl acetate (20 mL), washed with NaHCO<sub>3</sub> (10 mL) and brine (5 mL), and dried over MgSO<sub>4</sub>. Flash silica gel chromatography using 1–10% MeOH in CH<sub>2</sub>Cl<sub>2</sub> gives the hydroxyl compound.

**1,1,1-Trifluoro-4-methylpent-3-en-2-one (2).** To a 0–5 °C mixture of *N,O*-dimethylhydroxylamine hydrochloride (15.8 g) in CH<sub>2</sub>Cl<sub>2</sub> (400 mL) was added dropwise trifluoroacetic anhydride (21.7 mL). Pyridine (37 mL) was added to the mixture dropwise. The resulting mixture was stirred at 0–5 °C for 0.5 h and diluted with water. The organic layer was washed with water, 1 N aqueous HCl, water, and brine, and dried (MgSO<sub>4</sub>). Removal of the volatiles in vacuo for 5 min provided 2,2,2-trifluoro-*N*-methoxy-*N*-methylacetamide as a colorless oil.

To a 0–5 °C mixture of 2,2,2-trifluoro-*N*-methoxy-*N*-methylacetamide (3 g) in anhydrous ether (30 mL) was added 2-methylpropenylmagnesium bromide in THF (42 mL of a 0.5 M solution). The mixture was stirred at 0–5 °C for 0.5 h, warmed to room temperature, and stirred overnight. The reaction was quenched with saturated aqueous NH<sub>4</sub>Cl and extracted with ether three times. The organic layers were combined and washed with water and brine and dried (MgSO<sub>4</sub>). Most of the volatiles were removed at atmospheric pressure, and the resulting ether/THF solution of **2** was used without further purification.

**1,1,1-Trifluoro-4-(5-fluoro-2-methoxyphenyl)-4-methylpentan-2-one (3).** Following the general Grignard reaction procedure using 5-fluoro-2-methoxyphenylmagnesium bromide yielded **3** (46%) as an oil.

**5-(5-Fluoro-2-methoxyphenyl)-5-methyl-3-trifluoromethylhex-1-yn-3-ol (4).** Following the general propargylation procedure using **3** as starting material afforded **4** as an oil (92% yield) which was carried on to the next step without further purification.

**1,1,1-Trifluoro-4-(5-fluoro-2-methoxyphenyl)-4-methyl-2-(1*H*-pyrrolo[2,3-*b*]pyridin-2-ylmethyl)pentan-2-ol (5).** Following the general Sonogashira coupling procedure starting from **4** and (3-iodopyridin-2-yl)carbamic acid *tert*-butyl ester,<sup>14b</sup> which was prepared via Boc-protection and iodination of 2-aminopyridine, gave {3-[6-(5-fluoro-2-methoxyphenyl)-4-hydroxy-6-methyl-4-trifluoromethylhept-1-ynyl]pyridin-2-yl}carbamic acid *tert*-butyl ester (39% yield).

Following the general Boc-deprotection procedure starting from {3-[6-(5-fluoro-2-methoxyphenyl)-4-hydroxy-6-methyl-4-trifluoromethylhept-1-ynyl]pyridin-2-yl}carbamic acid *tert*-butyl ester gave 1-(2-aminopyridin-3-yl)-6-(5-fluoro-2-methoxyphenyl)-6-methyl-4-trifluoromethylhept-1-yn-4-ol, which was carried on to the next step without purification (assumed quantitative yield).

Following the general cyclization procedure A starting from 1-(4-aminopyridin-3-yl)-6-(5-fluoro-2-methoxyphenyl)-6-methyl-4-trifluoromethylhept-1-yn-4-ol gave **5** as a white solid (yield 13% over two steps). <sup>1</sup>H NMR (400 MHz, MeOH-*d*<sub>4</sub>)  $\delta$  8.06 (d, *J* = 4.24 Hz, 1H), 7.82 (dd, *J* = 7.89 Hz, *J* = 1.27 Hz, 1H), 7.06

(dd,  $J = 10.91$  Hz,  $J = 2.57$  Hz, 1H), 7.01 (dd,  $J = 7.89$  Hz,  $J = 4.86$  Hz, 1H), 6.91–6.83 (m, 2H), 6.09 (s, 1H), 3.76 (s, 3H), 2.95 (d,  $J = 15.31$  Hz, 1H), 2.85 (d,  $J = 15.31$  Hz, 1H), 2.60 (d,  $J = 15.31$  Hz, 1H), 2.14 (d,  $J = 15.31$  Hz, 1H), 1.57 (s, 3H), 1.38 (s, 3H); HPLC (system 1) purity 95%,  $t_R = 10.28$  min. LC–MS (system 2a):  $m/z = 411.4$  (M + H)<sup>+</sup>,  $t_R = 7.40$  min.

**1,1,1-Trifluoro-4-(5-fluoro-2-methoxyphenyl)-4-methyl-2-(1H-pyrrolo[2,3-c]pyridin-2-ylmethyl)pentan-2-ol (6).** Following the general Sonogashira coupling procedure starting from **4** and (4-iodopyridin-3-yl)carbamic acid *tert*-butyl ester<sup>14c</sup> gave {4-[6-(5-fluoro-2-methoxyphenyl)-4-hydroxy-6-methyl-4-trifluoromethylhept-1-ynyl]pyridin-3-yl}carbamic acid *tert*-butyl ester (78% yield).

Following the general Boc-deprotection procedure starting from {4-[6-(5-fluoro-2-methoxyphenyl)-4-hydroxy-6-methyl-4-trifluoromethylhept-1-ynyl]pyridin-3-yl}carbamic acid *tert*-butyl ester gave 1-(3-aminopyridin-4-yl)-6-(5-fluoro-2-methoxyphenyl)-6-methyl-4-trifluoromethylhept-1-yn-4-ol which was carried on to the next step without purification (assumed quantitative yield).

Following the general cyclization procedure A starting from 1-(3-aminopyridin-4-yl)-6-(5-fluoro-2-methoxyphenyl)-6-methyl-4-trifluoromethylhept-1-yn-4-ol gave **6** as a white solid (yield 43% over two steps). <sup>1</sup>H NMR (400 MHz, MeOH-*d*<sub>4</sub>)  $\delta$  8.53 (s, 1H), 7.95 (d,  $J = 5.56$  Hz, 1H), 7.42 (dd,  $J = 5.56$  Hz,  $J = 0.84$  Hz, 1H), 7.08 (dd,  $J = 11.78$  Hz,  $J = 1.60$  Hz, 1H), 6.90 (d,  $J = 6.30$  Hz, 1H), 6.89 (d,  $J = 6.90$  Hz, 1H), 6.16 (s, 1H), 3.78 (s, 3H), 2.98 (d,  $J = 15.31$  Hz, 1H), 2.86 (d,  $J = 15.31$  Hz, 1H), 2.61 (d,  $J = 15.31$  Hz, 1H), 2.13 (d,  $J = 15.31$  Hz, 1H), 1.59 (s, 3H), 1.39 (s, 3H); HPLC (system 1) purity 98%,  $t_R = 9.76$  min. LC–MS (system 2b):  $m/z = 411.2$  (M + H)<sup>+</sup>,  $t_R = 1.33$  min.

(*R*)-**6**. Resolution to the (+)- and (–)-enantiomers was accomplished by chiral HPLC on a CHIRALCEL OD column, eluting with 15–25% isopropanol–hexanes (>98 ee). The absolute configuration was determined by chiral HPLC comparison with (*R*)-**6** which was accessed from (*R*)-**4**.<sup>15</sup>

**1,1,1-Trifluoro-4-(5-fluoro-2-methoxyphenyl)-4-methyl-2-(1H-pyrrolo[3,2-c]pyridin-2-ylmethyl)pentan-2-ol (7).** Following the general Sonogashira coupling procedure starting from **4** and (3-iodopyridin-4-yl)carbamic acid *tert*-butyl ester<sup>14d</sup> gave {3-[6-(5-fluoro-2-methoxyphenyl)-4-hydroxy-6-methyl-4-trifluoromethylhept-1-ynyl]pyridin-4-yl}carbamic acid *tert*-butyl ester (yield 93%).

Following the general Boc-deprotection procedure starting from {3-[6-(5-fluoro-2-methoxyphenyl)-4-hydroxy-6-methyl-4-trifluoromethylhept-1-ynyl]pyridin-4-yl}carbamic acid *tert*-butyl ester gave 1-(4-aminopyridin-3-yl)-6-(5-fluoro-2-methoxyphenyl)-6-methyl-4-trifluoromethylhept-1-yn-4-ol, which was carried on to the next step without purification (assumed quantitative yield).

Following the general cyclization procedure A starting from 1-(3-aminopyridin-4-yl)-6-(5-fluoro-2-methoxyphenyl)-6-methyl-4-trifluoromethylhept-1-yn-4-ol gave **7** as a white solid (yield 35% over two steps). <sup>1</sup>H NMR (400 MHz, MeOH-*d*<sub>4</sub>)  $\delta$  8.61 (s, 1H), 8.03 (d,  $J = 5.77$  Hz, 1H), 7.34 (d,  $J = 5.77$  Hz, 1H), 7.08 (d,  $J = 10.77$  Hz, 1H), 6.90 (d,  $J = 6.15$  Hz, 1H), 6.89 (d,  $J = 6.15$  Hz, 1H), 6.23 (s, 1H), 3.79 (s, 3H), 2.99 (d,  $J = 15.31$  Hz, 1H), 2.83 (d,  $J = 15.31$  Hz, 1H), 2.58 (d,  $J = 15.31$  Hz, 1H), 2.12 (d,  $J = 15.31$  Hz, 1H), 1.59 (s, 3H), 1.34 (s, 3H); HPLC (system 1) purity >99%,  $t_R = 11.14$  min. LC–MS (system 2a):  $m/z = 411.2$  (M + H)<sup>+</sup>,  $t_R = 6.31$  min.

(*R*)-**7** can be accessed from (*R*)-**4** (>98% ee).<sup>15</sup>

**1,1,1-Trifluoro-4-(5-fluoro-2-methoxyphenyl)-4-methyl-2-(1H-pyrrolo[3,2-*b*]pyridin-2-ylmethyl)pentan-2-ol (8).** Following the general Sonogashira coupling procedure starting from **4** and (2-bromopyridin-3-yl)carbamic acid *tert*-butyl ester<sup>14e</sup> gave {2-[6-(5-fluoro-2-methoxyphenyl)-4-hydroxy-6-methyl-4-trifluoromethylhept-1-ynyl]pyridin-3-yl}carbamic acid *tert*-butyl ester (yield 58%).

{2-[6-(5-Fluoro-2-methoxyphenyl)-4-hydroxy-6-methyl-4-trifluoromethylhept-1-ynyl]pyridin-3-yl}carbamic acid *tert*-butyl ester (0.81 mmol) in 5 mL of HCl in ethyl acetate was stirred at room temperature for 48 h. Then the solvent was removed in vacuo and the residual solid washed with ether and dried to yield **8** as a white solid (99% yield). <sup>1</sup>H NMR (400 MHz, MeOH-*d*<sub>4</sub>)  $\delta$  8.37 (d,  $J = 6.32$  Hz, 1H), 8.35 (d,  $J = 8.38$  Hz, 1H), 7.52 (dd,  $J = 8.38$  Hz,  $J = 6.32$  Hz, 1H), 7.10 (dd,  $J = 10.59$  Hz,  $J = 3.00$  Hz, 1H), 6.97–6.90 (m, 2H), 6.48 (s, 1H), 3.87 (s, 3H), 3.12 (d,  $J = 15.31$  Hz, 1H), 2.94 (d,  $J = 15.31$  Hz, 1H), 2.62 (d,  $J = 15.31$  Hz, 1H), 2.05 (d,  $J = 15.31$  Hz, 1H), 1.67 (s, 3H), 1.42 (s, 3H); HPLC (system 1) purity 99%,  $t_R = 9.56$  min. LC–MS (system 2a):  $m/z = 411.6$  (M + H)<sup>+</sup>,  $t_R = 6.21$  min.

**1,1,1-Trifluoro-4-(5-fluoro-2-methoxyphenyl)-4-methyl-2-(6-oxo-1H-pyrrolo[2,3-c]pyridin-2-ylmethyl)pentan-2-ol (9).** To a solution of 1,1,1-trifluoro-4-(5-fluoro-2-methoxyphenyl)-4-methyl-2-(1H-pyrrolo[2,3-c]pyridin-2-ylmethyl)pentan-2-ol (**6**) (0.36 mmol) in dimethoxyethane (5 mL) was added *m*-chloroperbenzoic acid (0.54 mmol), and the mixture was stirred for 2 h. The solvent was then evaporated and the remaining oil dissolved in ethyl acetate (20 mL) and washed with NaHCO<sub>3</sub> (2 × 10 mL). The combined aqueous layers were extracted with ethyl acetate (2 × 10 mL) and the combined organic layers washed with brine, dried over MgSO<sub>4</sub>, and concentrated. Flash silica gel chromatography using 2–10% MeOH in CH<sub>2</sub>Cl<sub>2</sub> gave **9** (41% yield). <sup>1</sup>H NMR (400 MHz, MeOH-*d*<sub>4</sub>)  $\delta$  8.46 (s, 1H), 7.89 (dd,  $J = 6.86$  Hz,  $J = 1.70$  Hz, 1H), 7.51 (d,  $J = 6.86$  Hz, 1H), 7.09–7.06 (m, 1H), 6.92–6.89 (m, 2H), 6.25 (s, 1H), 3.82 (s, 3H), 3.07 (d,  $J = 15.31$  Hz, 1H), 2.83 (d,  $J = 15.31$  Hz, 1H), 2.55 (d,  $J = 15.31$  Hz, 1H), 2.07 (d,  $J = 15.31$  Hz, 1H), 1.62 (s, 3H), 1.39 (s, 3H); HPLC (system 1) purity 91%,  $t_R = 10.25$  min. LC–MS (system 2a):  $m/z = 427.6$  (M + H)<sup>+</sup>,  $t_R = 7.04$  min.

**2-[2-(5-Fluoro-2-methoxyphenyl)-2-methylpropyl]-2-trifluoromethylloxirane (10).** To a suspension of trimethylsulfoxonium iodide (4.76 g; 21.5 mmol) in DMSO (25 mL) was added NaH (0.863 g of a 60% dispersion in oil, 21.5 mmol) in four portions. After being stirred for 0.5 h, the solution was added to **3** (5.00 g, 17.9 mmol) in DMSO (20 mL). After 2 h the mixture was diluted with water (150 mL) and extracted with ether (2 × 125 mL). The combined organic layers were washed with water, brine and dried (MgSO<sub>4</sub>). Removal of the volatiles in vacuo provided **10** as an oil which was used without further purification.

**1,1,1-Trifluoro-4-(5-fluoro-2-methoxyphenyl)-2-furo[2,3-c]pyridin-2-ylmethyl-4-methylpentan-2-ol (11).** An inseparable mixture of 2-methylfuro[2,3-c]pyridine (0.81 mmol) and 2-methylfuro[3,2-*b*]pyridine (1.22 mmol) in 2 mL of THF was treated with lithium diisopropylamide (LDA; 1.5 M in cyclohexane, 1.58 mL) dropwise at –78 °C. The mixture was stirred for 30 min and was slowly treated with a solution of 1,1,1-trifluoro-4-(5-fluoro-2-methoxyphenyl)-4-methylpentan-2-one (**3**) (2.84 mmol) in 1 mL of THF. The mixture was stirred at –78 °C for 2 h, was then allowed to slowly warm to room temperature, and was stirred overnight. The reaction was quenched with 5 mL of NH<sub>4</sub>Cl, diluted with ethyl acetate (20 mL), and the aqueous layer was extracted with ethyl acetate (3 × 10 mL). The combined organic layers were washed with brine, dried over MgSO<sub>4</sub>, and concentrated. Flash chromatography using 0–50% ethyl acetate in hexanes gave pure **11** (yield 18%). The mixed fractions of the two isomers were not further purified. <sup>1</sup>H NMR (400 MHz, CDCl<sub>3</sub>)  $\delta$  8.76 (s, 1H), 8.35 (d,  $J = 5.30$  Hz, 1H), 7.42 (d,  $J = 5.30$  Hz, 1H), 7.09 (dd,  $J = 10.65$  Hz,  $J = 3.08$  Hz, 1H), 6.92–6.87 (m, 1H), 6.77 (dd,  $J = 9.02$  Hz,  $J = 4.81$  Hz, 1H), 6.46 (s, 1H), 3.77 (s, 3H), 2.98 (d,  $J = 15.31$  Hz, 1H), 2.90 (d,  $J = 15.31$  Hz, 1H), 2.67 (d,  $J = 15.31$  Hz, 1H), 2.44 (d,  $J = 15.31$  Hz, 1H), 1.54 (s, 3H), 1.45 (s, 3H); HPLC (system 1) purity 95%,  $t_R = 9.46$  min; ES-MS  $m/z = 412.5$  (M + H)<sup>+</sup>.

**1,1,1-Trifluoro-4-(5-fluoro-2-methoxyphenyl)-2-furo[2,3-c]pyridin-2-ylmethyl-4-methylpentan-2-ol (12).** A solution of thieno[2,3-*c*]pyridine (0.44 mmol) in 2 mL of THF was treated with <sup>t</sup>BuLi (1.7 M, 0.44 mmol) in a dropwise manner at –78 °C. The

resulting dark reaction mixture was stirred for 20 min and then treated with a solution of 2-[2-(5-fluoro-2-methoxyphenyl)-2-methylpropyl]-2-trifluoromethyloxirane (**6**) (0.34 mmol) in 0.5 mL of THF. The mixture was allowed to warm to room temperature overnight and quenched with a mixture of 5 mL of ammonium chloride and diluted with 10 mL of ethyl acetate. Phases were separated, and the aqueous layer was extracted with three 10 mL portions of ethyl acetate. The combined organic layers were washed with brine, dried over MgSO<sub>4</sub>, and concentrated in vacuo. Flash chromatography using 25% ethyl acetate in hexane gave **12** (11% yield) as a white solid. <sup>1</sup>H NMR (400 MHz, CDCl<sub>3</sub>): δ 9.04 (sbr, 1H), 8.46 (sbr, 1H), 7.57 (d, *J* = 4.51 Hz, 1H), 7.07 (dd, *J* = 10.76 Hz, *J* = 3.09 Hz, 1H), 7.05 (s, 1H), 6.94–6.89 (m, 1H), 6.76 (dd, *J* = 9.06 Hz, *J* = 4.71 Hz, 1H), 3.71 (s, 3H), 3.13 (sbr, 2H), 2.55 (d, *J* = 15.31 Hz, 1H), 2.46 (d, *J* = 15.31 Hz, 1H), 1.50 (s, 3H), 1.40 (s, 3H). LC–MS (system 2a): *m/z* = 428.6 (M + H)<sup>+</sup>, purity 95%, *t<sub>R</sub>* = 6.55 min.

**1,1,1-Trifluoro-4-(5-fluoro-2-methoxyphenyl)-4-methyl-2-pyrrolo[3,2-*b*]pyridin-1-ylmethylpentan-2-ol (13)**. A solution of 1*H*-pyrrolo[3,2-*b*]pyridine (0.28 mmol) in 4 mL of DMF was treated with NaH (0.42 mmol) at room temperature. After 30 min, **10** (0.56 mmol) was added and the resulting mixture was stirred overnight. Then the mixture was diluted with 5 mL of ethyl acetate and quenched with 5 mL of NH<sub>4</sub>Cl. The aqueous layer was extracted with 5 mL of ethyl acetate. The combined organic layers were dried over MgSO<sub>4</sub>, filtered, and concentrated in vacuo. Trituration with diethyl ether afforded **13** (30% yield) as a crystalline white solid. <sup>1</sup>H NMR (400 MHz, MeOH-*d*<sub>4</sub>): δ 8.22 (dd, *J* = 4.74 Hz, *J* = 1.34 Hz, 1H), 7.48 (d, *J* = 8.32 Hz, 1H), 7.36 (d, *J* = 3.36 Hz, 1H), 7.19 (ddd, *J* = 10.68 Hz, *J* = 2.52 Hz, *J* = 0.88 Hz, 1H), 7.10 (dd, *J* = 8.36 Hz, *J* = 4.76 Hz, 1H), 6.99–6.92 (m, 2H), 6.50 (dd, *J* = 3.36 Hz, *J* = 0.80 Hz, 1H), 4.00 (dq, *J* = 15.40 Hz, *J* = 1.62 Hz, 1H), 3.92 (d, *J* = 15.44 Hz, 1H), 3.85 (s, 3H), 2.94 (d, *J* = 15.28 Hz, 1H), 2.17 (d, *J* = 15.20 Hz, 1H), 1.66 (s, 3H), 1.43 (s, 3H). LC–MS (system 2b): *m/z* = 411.4 (M + H)<sup>+</sup>, 98% purity, *t<sub>R</sub>* = 1.36 min.

**1,1,1-Trifluoro-4-(5-fluoro-2-methoxyphenyl)-4-methyl-2-pyrrolo[2,3-*c*]pyridin-1-ylmethylpentan-2-ol (14)**. Following the same procedure as described for **13** using 1*H*-pyrrolo[2,3-*c*]pyridine (0.93 mmol) as starting material and preparative thin layer chromatography using 10% MeOH in CH<sub>2</sub>Cl<sub>2</sub> for purification afforded **14** (6% yield) as a white solid. <sup>1</sup>H NMR (400 MHz, CDCl<sub>3</sub>) δ 8.49 (s, 1H), 8.04 (d, *J* = 5.76 Hz, 1H), 7.62 (d, *J* = 5.76 Hz, 1H), 7.43 (d, *J* = 3.01 Hz, 1H), 7.20 (dd, *J* = 10.56 Hz, *J* = 2.78 Hz, 1H), 7.00–6.92 (m, 2H), 6.55 (d, *J* = 3.01 Hz, 1H), 4.11 (d, *J* = 15.31 Hz, 1H), 4.01 (d, *J* = 15.31 Hz, 1H), 3.88 (s, 3H), 2.89 (d, *J* = 15.31 Hz, 1H), 2.18 (d, *J* = 15.31 Hz, 1H), 1.67 (s, 3H), 1.44 (s, 3H); HPLC (system 1) purity 99%, *t<sub>R</sub>* = 9.53 min; ES-MS *m/z* = 411.5 (M + H)<sup>+</sup>.

**1,1,1-Trifluoro-4-(5-fluoro-2-methoxyphenyl)-4-methyl-2-pyrazolo[1,5-*a*]pyridin-2-ylmethylpentan-2-ol (15)**. Following the general Sonogashira coupling procedure using **4** and 2-iodopyridine yielded 6-(5-fluoro-2-methoxyphenyl)-6-methyl-1-pyridin-2-yl-4-trifluoromethylhept-1-yn-4-ol (43% yield).

To a solution of 6-(5-fluoro-2-methoxyphenyl)-6-methyl-1-pyridin-2-yl-4-trifluoromethylhept-1-yn-4-ol (0.40 mmol) and ethyl *O*-mesitylsulfonylacetohydroxamate (0.67 mmol) in dioxane (2 mL) was added perchloric acid (1.39 mmol) at 0 °C. The mixture was allowed to slowly warm up to room temperature and stirred for 4 days and the solvent removed. To the crude product in DMF (2 mL) was added K<sub>2</sub>CO<sub>3</sub> (1.17 mmol) and the reaction stirred at room temperature for 12 h. The reaction mixture was diluted with water (5 mL) and extracted with ethyl acetate (3 × 5 mL). The organic layers were combined, dried over MgSO<sub>4</sub>, and concentrated. Preparative thin layer chromatography using 25% ethyl acetate in hexanes gave **15** (17% yield) as a white solid. <sup>1</sup>H NMR (400 MHz, CDCl<sub>3</sub>) δ 8.31 (d, *J* = 7.05 Hz, 1H), 7.41 (d, *J* = 8.89 Hz, 1H), 7.10–7.06 (m, 2H), 6.85–6.81 (m, 1H), 6.73–6.69 (m, 2H), 6.17 (s, 1H), 3.79 (s, 3H), 2.89 (d, *J* = 15.31 Hz, 1H), 2.87 (d, *J* = 15.31 Hz, 1H), 2.66

(d, *J* = 15.31 Hz, 1H), 2.18 (d, *J* = 15.31 Hz, 1H), 1.62 (s, 3H), 1.41 (s, 3H). LC–MS (system 2a): *m/z* = 411.6 (M + H)<sup>+</sup>, purity 95%, *t<sub>R</sub>* = 8.74 min.

**4-Fluoro-2-[(*R*)-4,4,4-trifluoro-3-hydroxy-1,1-dimethyl-3-(1*H*-pyrrolo[2,3-*c*]pyridin-2-ylmethyl)butyl]phenol ((*R*)-16)**. Following the general demethylation procedure using (*R*)-**5** as starting material gave the desired product (*R*)-**16** (80% yield) as pale yellow crystals. <sup>1</sup>H NMR (400 MHz, DMSO-*d*<sub>6</sub>) δ 11.21 (s, 1H), 9.65 (s, 1H), 8.69 (s, 1H), 8.04 (d, *J* = 5.15 Hz, 1H), 7.44 (d, *J* = 5.10 Hz, 1H), 7.01 (dd, *J* = 2.79 Hz, *J* = 10.93 Hz, 1H), 6.88 (m, 1H), 6.80 (dd, *J* = 5.09 Hz, *J* = 8.80 Hz, 1H), 6.22 (s, 1H), 6.01 (s, 1H), 5.80 (d, *J* = 0.92 Hz, 1H), 3.11 (d, *J* = 15.11 Hz, 1H), 2.85 (d, *J* = 15.25 Hz, 1H), 2.58 (d, *J* = 15.17 Hz, 1H), 2.08 (d, *J* = 15.05 Hz, 1H), 1.61 (s, 3H), 1.41 (s, 3H); HPLC (system 1) purity 99%, *t<sub>R</sub>* = 9.15 min. LC–MS (system 2a): *m/z* = 397.6 (M + H)<sup>+</sup>, *t<sub>R</sub>* = 5.94 min; >98% ee. HRMS: *m/z* = 397.15311 (mass error 0.65 ppm) (M + H)<sup>+</sup>.

**4-Fluoro-2-[(*R*)-4,4,4-trifluoro-3-hydroxy-1,1-dimethyl-3-(1*H*-pyrrolo[3,2-*c*]pyridin-2-ylmethyl)butyl]phenol ((*R*)-17)**. Following the general demethylation procedure using (*R*)-**6** as a starting material gave (*R*)-**17** (64% yield) as pale yellow solid. <sup>1</sup>H NMR (400 MHz, MeOH-*d*<sub>4</sub>) δ 8.61 (s, 1H), 8.02 (d, *J* = 6.03 Hz, 1H), 7.35 (d, *J* = 7.33 Hz, 1H), 7.01 (dd, *J* = 2.96 Hz, *J* = 11.05 Hz, 1H), 6.72 (m, 2H), 6.23 (s, 1H), 3.20 (d, *J* = 15.26 Hz, 1H), 2.87 (d, *J* = 15.26 Hz, 1H), 2.63 (d, *J* = 15.26 Hz, 1H), 2.04 (d, *J* = 15.22 Hz, 1H), 1.62 (s, 3H), 1.43 (s, 3H); HPLC (system 1) purity >99%, *t<sub>R</sub>* = 8.97 min; ES-MS *m/z* = 397.1 (M + H)<sup>+</sup>; >98% ee.

**1,1,1-Trifluoro-4-methyl-4-phenylpentan-2-one (22)**. Following the general Grignard procedure using phenylmagnesium chloride (**18**) (2 M in THF) gave the desired product in 42% yield.

**1,1,1-Trifluoro-4-methyl-4-(3-fluorophenyl)pentan-2-one (23)**. Following the general Grignard reaction procedure using 3-fluorophenylmagnesium bromide (**19**) as a starting material gave **23** (78% yield) as a clear oil.

**1,1,1-Trifluoro-4-(5-fluoro-2-methylphenyl)-4-methylpentan-2-one (24)**. Following the general Grignard reaction procedure using 3-fluorophenylmagnesium bromide (**20**) as a starting material gave **24** (84% yield) as a clear oil.

**1,1,1-Trifluoro-4-(2-methoxyphenyl)-4-methylpentan-2-one (25)**. Following the general Grignard reaction procedure using a freshly prepared Grignard reagent **21** from 2-bromoanisole as a starting material gave the desired ketone **25** (44% yield).

**1,1,1-Trifluoro-4-(5-bromo-2-methoxyphenyl)-4-methylpentan-2-one (26)**. **25** (34.5 mmol) and *N*-bromosuccinimide (40 mmol) in CCl<sub>4</sub> (100 mL) were heated to reflux for 20 h. The solvent was removed, and hexanes (500 mL) were added. The mixture was filtered and the filtrate concentrated. The residue was purified by flash chromatography on silica gel using ethyl acetate in hexanes (0–20%) as eluent to yield **26** as a solid (73% yield).

**6-Methyl-6-phenyl-4-trifluoromethylhept-1-yn-4-ol (27)**. Following the general propargylation procedure using **22** as starting material gave **27** (94% yield) which was carried on to the next step without further purification.

**6-(3-Fluorophenyl)-6-methyl-4-trifluoromethylhept-1-yn-4-ol (28)**. Following the general propargylation procedure using **23** as a starting material gave **28** (94% yield) which was carried on to the next step without further purification.

**6-(5-Fluoro-2-methylphenyl)-6-methyl-4-trifluoromethylhept-1-yn-4-ol (29)**. Following the general propargylation procedure using **24** as a starting material gave **29** (99% yield) which was carried on to the next step without further purification.

**5-(5-Bromo-2-methoxyphenyl)-5-methyl-3-trifluoromethylhex-1-yn-3-ol (30)**. Following the same general propargylation procedure using **26** as a starting material yielded **30** (97% yield) as an oil.

**1,1,1-Trifluoro-4-methyl-4-phenyl-2-(1*H*-pyrrolo[2,3-*c*]pyridin-2-ylmethyl)pentan-2-ol (31)**. Following the general Sonogashira coupling procedure using **27** and (4-iodopyridin-3-yl)carbamic

acid *tert*-butyl ester<sup>14c</sup> as a starting materials and using 25–50% ethyl acetate in hexanes as eluent in the flash chromatography gave [4-(4-hydroxy-6-methyl-6-phenyl-4-trifluoromethylhept-1-ynyl)pyridin-3-yl]carbamic acid *tert*-butyl ester (78% yield) as a pale yellow solid.

Following the general Boc-deprotection procedure using [4-(4-hydroxy-6-methyl-6-phenyl-4-trifluoromethylhept-1-ynyl)pyridin-3-yl]carbamic acid *tert*-butyl ester as a starting material and stirring the mixture for 3 h gave 1-(3-aminopyridin-4-yl)-6-methyl-6-phenyl-4-trifluoromethylhept-1-yn-4-ol (assumed yield 100%) as the HCl salt.

Following the general cyclization procedure using 1-(3-aminopyridin-4-yl)-6-methyl-6-phenyl-4-trifluoromethylhept-1-yn-4-ol as starting material gave **31** (18% yield) as a white solid. <sup>1</sup>H NMR (400 MHz, MeOH-*d*<sub>4</sub>) δ 8.57 (s, 1H), 7.97 (d, *J* = 5.75 Hz, 1H), 7.50 (d, *J* = 5.75 Hz, 1H), 7.44 (m, 2H), 7.27 (m, 2H), 7.15 (m, 1H), 6.20 (s, 1H), 2.82 (d, *J* = 15.28 Hz, 1H), 2.47 (15.26 Hz, 2H), 2.17 (*J* = 15.26 Hz, 1H), 1.65 (s, 3H), 1.35 (s, 3H); HPLC (system 1) purity > 99%, *t*<sub>R</sub> = 9.20 min. LC–MS (system 2a): *m/z* = 363.6 (M + H)<sup>+</sup>, *t*<sub>R</sub> = 6.15 min.

**1,1,1-Trifluoro-4-(3-fluorophenyl)-4-methyl-2-(1*H*-pyrrolo[2,3-*c*]pyridin-2-ylmethyl)pentan-2-ol (32).** Following the general Sonogashira coupling procedure using 6-(3-fluorophenyl)-6-methyl-4-trifluoromethylhept-1-yn-4-ol (**28**) and (4-iodopyridin-3-yl)carbamic acid *tert*-butyl ester<sup>14c</sup> as a starting materials and using 15–50% ethyl acetate in hexanes as eluent in the flash chromatography gave the {4-[6-(3-fluorophenyl)-4-hydroxy-6-methyl-4-trifluoromethylhept-1-ynyl]phenyl}carbamic acid *tert*-butyl ester (54% yield) as a pale yellow solid.

Following the general Boc-deprotection procedure using {4-[6-(3-fluorophenyl)-4-hydroxy-6-methyl-4-trifluoromethylhept-1-ynyl]phenyl}carbamic acid *tert*-butyl ester as a starting material and stirring the mixture for 10 h gave 1-(3-aminopyridin-4-yl)-6-(3-fluorophenyl)-6-methyl-4-trifluoromethylhept-1-yn-4-ol (assumed yield 100%) as the HCl salt.

Following the general cyclization procedure A starting from 1-(3-aminopyridin-4-yl)-6-(3-fluorophenyl)-6-methyl-4-trifluoromethylhept-1-yn-4-ol and stirring for 3 days gave **32** (30% yield) as a white solid. <sup>1</sup>H NMR (400 MHz, MeOH-*d*<sub>4</sub>) δ 8.58 (s, 1H), 7.99 (s, 1H), 7.46 (d, *J* = 5.41 Hz, 1H), 7.20 (m, 3H), 6.88 (m, 1H), 6.23 (s, 1H), 2.88 (d, *J* = 15.29 Hz, 1H), 2.65 (d, *J* = 15.29 Hz, 1H), 2.43 (d, *J* = 15.32 Hz, 1H), 2.21 (d, *J* = 15.32 Hz, 1H), 1.61 (s, 3H), 1.37 (s, 3H); HPLC (system 1) purity > 99%, *t*<sub>R</sub> = 9.56 min. LC–MS (system 2a): *m/z* = 381.6 (M + H)<sup>+</sup>, *t*<sub>R</sub> = 6.19 min.

**1,1,1-Trifluoro-4-(5-fluoro-2-methylphenyl)-4-methyl-2-(1*H*-pyrrolo[2,3-*c*]pyridin-2-ylmethyl)pentan-2-ol (33).** Following the general Sonogashira coupling procedure using 6-(5-fluoro-2-methylphenyl)-6-methyl-4-trifluoromethylhept-1-yn-4-ol (**29**) and (4-iodopyridin-3-yl)carbamic acid *tert*-butyl ester<sup>14c</sup> as starting materials and using 15–30% ethyl acetate in hexanes as eluent in the flash chromatography gave {4-[6-(5-fluoro-2-methylphenyl)-4-hydroxy-6-methyl-4-trifluoromethylhept-1-ynyl]pyridin-3-yl}carbamic acid *tert*-butyl ester (78% yield) as a pale yellow foam.

Following the general Boc-deprotection procedure using {4-[6-(5-fluoro-2-methylphenyl)-4-hydroxy-6-methyl-4-trifluoromethylhept-1-ynyl]pyridin-3-yl}carbamic acid *tert*-butyl ester as a starting material and stirring the mixture for 4 h gave 1-(3-aminopyridin-4-yl)-6-(5-fluoro-2-methylphenyl)-6-methyl-4-trifluoromethylhept-1-yn-4-ol (assumed yield 100%) as the HCl salt.

Following the general cyclization procedure A starting from 1-(3-aminopyridin-4-yl)-6-(5-fluoro-2-methylphenyl)-6-methyl-4-trifluoromethylhept-1-yn-4-ol and stirring for 3 days gave **33** (57% yield) as a white solid. <sup>1</sup>H NMR (400 MHz, MeOH-*d*<sub>4</sub>) δ 8.60 (s, 1H), 8.01 (s, 1H), 7.51 (d, *J* = 5.33 Hz, 1H), 7.22 (d, *J* = 2.81 Hz, 1H), 7.19 (d, *J* = 2.81 Hz, 1H), 7.11 (dd, *J* = 8.22 Hz, *J* = 6.36 Hz, 1H), 6.84 (dt, *J* = 8.22 Hz, *J* = 2.81 Hz, 1H), 6.26 (s, 1H), 2.92 (d, *J* = 15.23 Hz, 1H), 2.73 (d, *J* = 15.45 Hz, 1H),

2.67 (d, *J* = 15.23 Hz, 1H), 2.50 (s, 3H), 2.17 (d, *J* = 15.45 Hz, 1H), 1.70 (s, 3H), 1.49 (s, 3H); HPLC (system 1) purity > 99%, *t*<sub>R</sub> = 9.82 min; ES-MS *m/z* = 395.4 (M + H)<sup>+</sup>.

**4-(5-Bromo-2-methoxyphenyl)-1,1,1-trifluoro-4-methyl-2-(1*H*-pyrrolo[2,3-*c*]pyridin-2-ylmethyl)pentan-2-ol (34).** Following the general Sonogashira coupling procedure using 5-(5-bromo-2-methoxyphenyl)-5-methyl-3-trifluoromethylhex-1-yn-3-ol (**21**) and (4-iodo-pyridin-3-yl)carbamic acid *tert*-butyl ester<sup>14c</sup> as starting materials gave {3-[6-(5-bromo-2-methoxyphenyl)-4-hydroxy-6-methyl-4-trifluoromethylhept-1-ynyl]pyridin-4-yl}carbamic acid *tert*-butyl ester (63% yield).

Following the general cyclization procedure B using {3-[6-(5-bromo-2-methoxyphenyl)-4-hydroxy-6-methyl-4-trifluoromethylhept-1-ynyl]pyridin-4-yl}carbamic acid *tert*-butyl ester as a starting material gave **34** (86% yield). We also noticed that the removal of methanol and addition of more water lead to precipitation of the desired compound, which can be isolated by filtration.

**General Suzuki Coupling Procedure.** All the solid reagents (4-(5-bromo-2-methoxyphenyl)-1,1,1-trifluoro-4-methyl-2-(1*H*-pyrrolo[2,3-*c*]pyridin-2-ylmethyl)pentan-2-ol **34** (0.212 mmol, 1 equiv), boronic acid (0.318 mmol, 1.5 equiv), Pd catalyst/ligand and base) are mixed in a sealed tube, which is capped, evacuated, and flushed with argon three times. The solvents DME (1.5 mL), MeOH (2.2 mL), and DMF (0.75 mL) are added, and the reaction mixture is heated to 80 °C overnight. The reaction mixture is diluted with ethyl acetate (5 mL), filtered through Celite, and concentrated. The crude product is purified by flash chromatography on silica gel using 1–5% MeOH in CH<sub>2</sub>Cl<sub>2</sub> as eluent.

**1,1,1-Trifluoro-4-(4-methoxybiphenyl-3-yl)-4-methyl-2-(1*H*-pyrrolo[2,3-*c*]pyridin-2-ylmethyl)pentan-2-ol (35).** Following the general Suzuki coupling procedure starting from **25** and using Pd(OAc)<sub>2</sub> (0.2 equiv), (2-dicyclohexylphosphino)biphenyl (0.4 equiv), and potassium fluoride (4 equiv) gave the desired product as a white solid (40% yield). <sup>1</sup>H NMR (400 MHz, MeOH-*d*<sub>4</sub>) δ 8.56 (s, 1H), 7.95 (d, *J* = 5.87 Hz, 1H), 7.58 (d, *J* = 2.23 Hz, 1H), 7.51 (m, 3H), 7.46 (dd, *J* = 2.20 Hz, *J* = 8.44 Hz, 1H), 7.36 (t, *J* = 7.72 Hz, 2H), 7.24 (m, 1H), 7.04 (d, *J* = 8.44 Hz, 1H), 6.24 (s, 1H), 3.88 (s, 3H), 3.11 (d, *J* = 15.15 Hz, 1H), 2.94 (d, *J* = 15.15 Hz, 1H), 2.63 (d, *J* = 15.42 Hz, 1H), 2.13 (d, *J* = 15.42 Hz, 1H), 1.72 (s, 3H), 1.46 (s, 3H). LC–MS (system 2b) = 469.4 (M + H)<sup>+</sup>, purity 96%, *t*<sub>R</sub> = 1.52 min.

**1,1,1-Trifluoro-4-(2-methoxy-5-pyridin-3-ylphenyl)-4-methyl-2-(1*H*-pyrrolo[2,3-*c*]pyridin-2-ylmethyl)pentan-2-ol (36).** Following the general Suzuki coupling procedure starting from **34** using Pd(PPh<sub>3</sub>)<sub>4</sub> (0.1 equiv) and K<sub>2</sub>CO<sub>3</sub> (3 equiv) gave **36** as a white foam (45% yield). <sup>1</sup>H NMR (400 MHz, MeOH-*d*<sub>4</sub>) δ 8.69 (d, *J* = 1.89 Hz, 1H), 8.51 (sbr, 1H), 8.42 (dd, *J* = 1.42 Hz, *J* = 4.86 Hz, 1H), 7.97 (dt, *J* = 1.89 Hz, *J* = 7.96 Hz, 1H), 7.93 (d, *J* = 5.40 Hz, 1H), 7.59 (d, *J* = 2.23 Hz, 1H), 7.49 (dd, *J* = 2.23 Hz, *J* = 8.44 Hz, 1H), 7.43 (dd, *J* = 4.86 Hz, *J* = 7.96 Hz, 1H), 7.39 (d, *J* = 5.40 Hz, 1H), 7.06 (d, *J* = 8.44 Hz, 1H), 6.15 (s, 1H), 3.85 (s, 3H), 3.01 (d, *J* = 15.26 Hz, 1H), 2.91 (d, *J* = 15.12 Hz, 1H), 2.66 (d, *J* = 15.26 Hz, 1H), 2.19 (d, *J* = 15.12 Hz, 1H), 1.69 (s, 3H), 1.45 (s, 3H). LC–MS (system 2a) = 470.4 (M + H)<sup>+</sup>, purity 96%, *t*<sub>R</sub> = 5.61 min.

**1,1,1-Trifluoro-4-(2-methoxy-5-pyrimidin-5-ylphenyl)-4-methyl-2-(1*H*-pyrrolo[2,3-*c*]pyridin-2-ylmethyl)pentan-2-ol (37).** Following the general Suzuki coupling procedure using Pd(PPh<sub>3</sub>)<sub>4</sub> (0.1 equiv) and K<sub>2</sub>CO<sub>3</sub> (3 equiv) gave **37** as a white foam (33% yield). (*R*)-**37** was accessed starting with (*R*)-**30**. <sup>1</sup>H NMR (400 MHz, MeOH-*d*<sub>4</sub>) δ 9.05 (s, 1H), 8.97 (s, 2H), 8.53 (sbr, 1H), 7.94 (dbr, 1H), 7.63 (d, *J* = 2.29 Hz, 1H), 7.57 (dd, *J* = 2.29 Hz, *J* = 8.42 Hz, 1H), 7.43 (d, *J* = 5.27 Hz, 1H), 7.11 (d, *J* = 8.42 Hz, 1H), 6.19 (s, 1H), 3.88 (s, 3H), 3.02 (d, *J* = 15.53 Hz, 1H), 2.92 (d, *J* = 15.53 Hz, 1H), 2.69 (d, *J* = 15.25 Hz, 1H), 2.21 (d, *J* = 15.25 Hz, 1H), 1.71 (s, 3H), 1.46 (s, 3H). LC–MS (system 2a) = 471.6 (M + H)<sup>+</sup>, purity > 99%, *t*<sub>R</sub> = 4.55 min; > 98% ee. HRMS: *m/z* = 471.20022 (mass error 0.005 ppm) (M + H)<sup>+</sup>,

**3-[4,4,4-Trifluoro-3-hydroxy-1,1-dimethyl-3-(1*H*-pyrrolo[2,3-*c*]pyridin-2-ylmethyl)butyl]biphenyl-4-ol (38).** Following the general demethylation procedure using **35** as a starting material gave **38** as an off-white solid (63% yield). <sup>1</sup>H NMR (400 MHz, MeOH-*d*<sub>4</sub>) δ 8.51 (sbr, 1H), 7.92 (dbr, 1H), 7.54 (d, *J* = 2.23 Hz, 1H), 7.48 (m, 2H), 7.40 (d, *J* = 5.81 Hz, 1H), 7.32 (m, 3H), 7.21 (t, *J* = 7.44 Hz, 1H), 6.84 (d, *J* = 8.21 Hz, 1H), 6.14 (s, 1H), 3.24 (d, *J* = 15.14 Hz, 1H), 2.98 (d, *J* = 15.14 Hz, 1H), 2.71 (d, *J* = 15.14 Hz, 1H), 2.10 (d, *J* = 15.14 Hz, 1H), 1.72 (s, 3H), 1.50 (s, 3H). LC-MS (system 2a) = 455.6 (M + H)<sup>+</sup>, purity 95%, *t*<sub>R</sub> = 6.32 min.

**4-Pyridin-3-yl-2-[4,4,4-trifluoro-3-hydroxy-1,1-dimethyl-3-(1*H*-pyrrolo[2,3-*c*]pyridin-2-ylmethyl)butyl]phenol (39).** Following the general demethylation procedure using **36** as starting material gave the desired product as a white solid (29% yield). <sup>1</sup>H NMR (400 MHz, MeOH-*d*<sub>4</sub>) δ 8.65 (d, *J* = 1.52 Hz, 1H), 8.58 (s, 1H), 8.39 (d, *J* = 4.36 Hz, 1H), 7.96 (m, 2H), 7.55 (d, *J* = 2.37 Hz, 1H), 7.53 (d, *J* = 5.88 Hz, 1H), 7.42 (dd, *J* = 4.86 Hz, *J* = 7.90 Hz, 1H), 7.36 (dd, *J* = 2.27 Hz, *J* = 8.34 Hz, 1H), 6.90 (d, *J* = 8.34 Hz, 1H), 6.26 (s, 1H), 3.28 (d, *J* = 15.34 Hz, 1H), 2.99 (d, *J* = 15.34 Hz, 1H), 2.72 (d, *J* = 15.15 Hz, 1H), 2.10 (d, *J* = 15.15 Hz, 1H), 1.74 (s, 3H), 1.50 (s, 3H). LC-MS (system 2b) = 456.4 (M + H)<sup>+</sup>, purity >95%, *t*<sub>R</sub> = 0.90 min.

**4-Bromo-2-[4,4,4-trifluoro-3-hydroxy-1,1-dimethyl-3-(1*H*-pyrrolo[2,3-*c*]pyridin-2-ylmethyl)butyl]phenol (40).** Following the general demethylation procedure using **34** as a starting material gave **40** as a white solid (87% yield).

**4-Pyrimidin-5-yl-2-[4,4,4-trifluoro-3-hydroxy-1,1-dimethyl-3-(1*H*-pyrrolo[2,3-*c*]pyridin-2-ylmethyl)butyl]phenol (41).** Following the general Suzuki coupling procedure using **40** instead of **25** and Pd(PPh<sub>3</sub>)<sub>4</sub> (0.1 equiv) and K<sub>2</sub>CO<sub>3</sub> (3 equiv) gave the desired product **41** as a white foam (2% yield). <sup>1</sup>H NMR (400 MHz, MeOH-*d*<sub>4</sub>) δ 9.02 (s, 1H), 8.94 (s, 2H), 8.55 (sbr, 1H), 7.94 (sbr, 1H), 7.59 (d, *J* = 2.25 Hz, 1H), 7.48 (sbr, 1H), 7.43 (dd, *J* = 2.25 Hz, *J* = 8.28 Hz, 1H), 6.94 (d, *J* = 8.28 Hz, 1H), 6.21 (s, 1H), 3.26 (d, *J* = 15.25 Hz, 1H), 2.97 (d, *J* = 15.12 Hz, 1H), 2.73 (d, 15.25 Hz, 1H), 2.13 (d, *J* = 15.12 Hz, 1H), 1.75 (s, 3H), 1.51 (s, 3H). LC-MS (system 2b) = 457.3 (M + H)<sup>+</sup>, purity >95%, *t*<sub>R</sub> = 1.11 min.

**2-Hydroxy-4-methyl-2-trifluoromethylpent-4-enoic Acid Ethyl Ester (44).** A 5 L three-neck round-bottom flask equipped with an overhead stirrer was charged with ethyl trifluoropyruvate (**42**) (0.764 mol) and THF (2 L). The solution was cooled to -65 °C, and methylallylmagnesium chloride (**43**) (1 mol, 0.5 M in THF) was added over 4 h, keeping the internal temperature below -60 °C. Then the mixture was allowed to warm to room temperature and stirred overnight. The solvent was then removed, and a saturated NH<sub>4</sub>Cl solution (1 L) was added and extracted with ether (3 × 1 L). The combined organic phases were washed with brine (100 mL), dried over MgSO<sub>4</sub>, and concentrated. Vacuum distillation of the product at 35–45 °C gave **44** (61% yield).

**4-(2,3-Dihydrobenzofuran-7-yl)-2-hydroxy-4-methyl-2-trifluoromethylpentanoic Acid Ethyl Ester (45).** To a solution of **44** (88 mmol) and dihydrobenzofurane (97 mmol) in dichloroethane (90 mL) was added aluminum chloride (130 mmol) at 0 °C, and the reaction mixture was stirred at room temperature overnight. The reaction mixture was poured into cold 1 N HCl (200 mL) and extracted with ethyl acetate (3 × 200 mL). The combined organic layers were washed with a saturated NaHCO<sub>3</sub> solution (200 mL) and brine (200 mL), dried over MgSO<sub>4</sub>, and concentrated. Flash chromatography on silica gel using 0–1% ethyl acetate in hexanes gave **45** (31% yield).

**4-(5-Fluoro-2,3-dihydrobenzofuran-7-yl)-2-hydroxy-4-methyl-2-trifluoromethylpentanoic Acid Ethyl Ester (46).** To a solution of 2,3-dihydrobenzofuran (0.212 mol) in acetic acid (175 mL) was added about one-quarter of 0.227 mol of 70% aqueous nitric acid dropwise. The reaction was monitored by TLC (EtOAc–hexanes (15:85)). The mixture was warmed to 70 °C where the reaction began. The remainder of the nitric acid was

then added while maintaining the reaction at 70 °C. After 30 min, the mixture was cooled and poured into 1.5 L of ice–water. The black solid was collected by filtration washing with water. The solid was partitioned between 500 mL of saturated aqueous sodium bicarbonate and 150 mL of EtOAc. The aqueous layer was separated and extracted with three 150 mL portions of EtOAc. The combined organic layers were washed with three 100 mL portions of saturated aqueous sodium bicarbonate, 100 mL of saturated aqueous ammonium chloride, and 100 mL of brine, dried over MgSO<sub>4</sub>, filtered, and concentrated to afford a red oil/solid. The mixture was dissolved in CH<sub>2</sub>Cl<sub>2</sub> and passed through a pad of silica gel, eluting with CH<sub>2</sub>Cl<sub>2</sub> and concentrated. The resulting red mixture was triturated with ether–hexanes (1:1) and filtered to afford of 5-nitro-2,3-dihydrobenzofuran (29% yield) as a tan solid.

To a suspension of 5-nitro-2,3-dihydrobenzofuran (62.37 mmol) in MeOH (50 mL) and CH<sub>2</sub>Cl<sub>2</sub> (10 mL) was added 10% palladium on carbon (350 mg), and the mixture was placed under 55 psi of hydrogen gas. Hydrogen gas uptake was evident during the first 30 min. After 18 h, the mixture was then filtered through diatomaceous earth and concentrated to afford 2,3-dihydrobenzofuran-5-ylamine (97%) as a gray solid which was used without further purification.

To a solution of 2,3-dihydrobenzofuran-5-ylamine (60.66 mmol) in THF (250 mL) was added 6 mL of concentrated aqueous HCl in several portions. To the resulting white precipitate was added dropwise tetrafluoroboric acid (11 mL). The mixture was then chilled (-15 °C), and sodium nitrite (68.12 mmol) in water (20 mL) was added dropwise. The suspension turned deep gray, became homogeneous, and then a precipitate formed. The mixture was stirred for 30 min at -15 °C, and then the solid was collected by filtration washing with cold water, cold ethanol, and cold ether. The solid was dried by pulling vacuum through the filter cake to afford 5-diazonium-2,3-dihydrobenzofuran tetrafluoroborate salt (68% yield) which was used without further purification.

A suspension of the above diazonium tetrafluoroborate salt (41.46 mmol) in xylenes was warmed at reflux for 1 h. The mixture was then cooled and diluted with 200 mL of saturated aqueous sodium bicarbonate. The aqueous layer was separated and extracted with three 50 mL portions of EtOAc. The combined organic layers were washed with 50 mL of aqueous sodium bicarbonate, 50 mL of brine, dried over MgSO<sub>4</sub>, filtered, and concentrated to afford an oil. The crude oil was chromatographed on silica gel using EtOAc–hexanes (0:100, then 0.5:99.5) to afford of 5-fluoro-2,3-dihydrobenzofuran (45% yield).

To a solution of **44** (20.33 mmol) and 5-fluoro-2,3-dihydrobenzofuran (18.82 mmol) in carbon disulfide (15 mL) was added in several portions aluminum trichloride (20.33 mmol). The mixture was stirred for 3 days (over which time the carbon disulfide had evaporated from the reaction mixture) and was then poured into cold 1 N aqueous HCl. The aqueous layer was extracted with ethyl acetate (3 × 30 mL). The combined organic layers were washed with 1 N aqueous HCl (2 × 20 mL), brine (20 mL), saturated aqueous sodium bicarbonate (2 × 20 mL), and brine (20 mL), dried over MgSO<sub>4</sub>, filtered, and concentrated. The thick oil was adsorbed onto silica gel and separated by flash chromatography on silica gel using ethyl acetate in hexanes (0–5%) to afford **46** as a solid (30% yield).

**4-(5-Chloro-2,3-dihydrobenzofuran-7-yl)-2-hydroxy-4-methyl-2-trifluoromethylpentanoic Acid Ethyl Ester (47).** To a solution of **45** (5.8 mmol) in acetic acid (20 mL) at 15 °C was added portionwise a solution of Cl<sub>2</sub> gas in acetic acid which was prepared by bubbling Cl<sub>2</sub> gas through acetic acid (~1 g of Cl<sub>2</sub> in 5 mL of acetic acid). After all the starting material was consumed, the mixture was made basic with saturated aqueous NaHCO<sub>3</sub>. The mixture was extracted with ethyl acetate (3 × 75 mL), the combined organic layers were washed with saturated aqueous NaHCO<sub>3</sub> solution (2 × 30 mL), brine (2 × 30 mL),

dried over  $\text{MgSO}_4$ , and concentrated. The crude product **47** was carried on to the next step without further purification.

**4-(2,3-Dihydrobenzofuran-7-yl)-1,1,1-trifluoro-4-methylpentan-2-one (48)**. To a mixture of **45** (98 mmol) in THF (330 mL) was added lithium aluminum hydride (98 mmol) in small portions. After 48 h the mixture was dropwise quenched with water at 0 °C,  $\text{MgSO}_4$  was added, and the mixture was filtered through Celite. The filtrate was concentrated in vacuo to leave 4-(2,3-dihydrobenzofuran-7-yl)-4-methyl-2-trifluoromethylpentane-1,2-diol as an oil (100% yield) which was carried on without further purification.

To a solution of 4-(2,3-dihydrobenzofuran-7-yl)-4-methyl-2-trifluoromethylpentane-1,2-diol (158 mmol) in MeOH (600 mL) was added sodium periodate (790 mmol), and the mixture was stirred overnight. The reaction mixture was filtered through Celite and the filtrate concentrated, taken up in hexanes, filtered again, and concentrated to afford **48** as a colorless oil (98% yield).

**1,1,1-Trifluoro-4-(5-fluoro-2,3-dihydrobenzofuran-7-yl)-4-methylpentan-2-one (49)**. Following the same reduction procedure as described for the conversion of **45** using **37** as starting material yielded 4-(5-fluoro-2,3-dihydrobenzofuran-7-yl)-4-methyl-2-trifluoromethylpentane-1,2-diol (98% yield) which was carried on to the next step without further purification.

Following the same procedure as described for **48** using 4-(5-fluoro-2,3-dihydrobenzofuran-7-yl)-4-methyl-2-trifluoromethylpentane-1,2-diol as a starting material and using 4.4 equiv of sodium periodate yielded **49** (95% yield) which was carried on without further purification.

**1,1,1-Trifluoro-4-(5-chloro-2,3-dihydrobenzofuran-7-yl)-4-methylpentan-2-one (50)**. Following the same reduction procedure as described for the conversion of **45** using **47** as a starting material yielded 4-(5-chloro-2,3-dihydrobenzofuran-7-yl)-4-methyl-2-trifluoromethylpentane-1,2-diol (43% yield) which was carried on to the next step without further purification.

Following the same procedure as described for **48** using 4-(5-chloro-2,3-dihydrobenzofuran-7-yl)-4-methyl-2-trifluoromethylpentane-1,2-diol as a starting material, using 3.5 equiv of sodium periodate, and filtration of the crude product through a pad of silica gel using hexanes as an eluent afforded **50** (90% yield).

**6-(2,3-Dihydrobenzofuran-7-yl)-6-methyl-4-trifluoromethylhept-1-yn-4-ol (51)**. Following the general propargylation procedure using **48** as a starting material gave **51** (95% yield), which was carried on to the next step without further purification.

**6-(5-Chloro-2,3-dihydrobenzofuran-7-yl)-6-methyl-4-trifluoromethylhept-1-yn-4-ol (52)**. Following the general propargylation procedure using **50** as a starting material gave **52** (64% yield) as a white solid.

**{4-[6-(2,3-Dihydrobenzofuran-7-yl)-4-hydroxy-6-methyl-4-trifluoromethylhept-1-ynyl]pyridin-3-yl}carbamic Acid tert-Butyl Ester (53)**. Following the general Sonogashira coupling procedure using **51** as a starting material and using 15–30% ethyl acetate in hexanes as eluent in the flash chromatography gave **53** (64% yield) as a white solid.

**{4-[6-(5-Chloro-2,3-dihydrobenzofuran-7-yl)-4-hydroxy-6-methyl-4-trifluoromethylhept-1-ynyl]pyridin-3-yl}carbamic Acid tert-Butyl Ester (54)**. Following the general Sonogashira coupling procedure using **52** as a starting material and using 15–30% ethyl acetate in hexanes as eluent in the flash chromatography gave **54** (73% yield) as a white solid.

**4-(2,3-Dihydrobenzofuran-7-yl)-1,1,1-trifluoro-4-methyl-2-(1H-pyrrolo[2,3-c]pyridin-2-ylmethyl)pentan-2-ol (55)**. Following the general Boc-deprotection procedure using **53** as a starting material and stirring the mixture for 4 h gave 1-(3-aminopyridin-4-yl)-6-(2,3-dihydrobenzofuran-7-yl)-6-methyl-4-trifluoromethylhept-1-yn-4-ol (assumed yield 100%) as the HCl salt.

Following the general cyclization procedure A starting from 1-(3-aminopyridin-4-yl)-6-(2,3-dihydrobenzofuran-7-yl)-6-methyl-4-trifluoromethylhept-1-yn-4-ol and stirring for 17 h gave **55**

(31% yield) as a white solid.  $^1\text{H NMR}$  (400 MHz,  $\text{MeOH}-d_4$ )  $\delta$  8.53 (s, 1H), 7.94 (d,  $J = 5.51$  Hz, 1H), 7.43 (d,  $J = 5.79$  Hz, 1H), 7.11 (d,  $J = 7.60$  Hz, 1H), 7.07 (dd,  $J = 1.21$  Hz,  $J = 7.24$  Hz, 1H), 6.78 (t,  $J = 7.60$  Hz, 1H), 6.15 (s, 1H), 4.49 (dt,  $J = 2.48$  Hz,  $J = 8.81$  Hz, 2H), 3.10 (dt,  $J = 2.48$  Hz,  $J = 8.81$  Hz, 2H), 2.95 (d,  $J = 15.16$  Hz, 1H), 2.89 (d,  $J = 15.33$  Hz, 1H), 2.56 (d,  $J = 15.33$  Hz, 1H), 2.04 (d,  $J = 15.16$  Hz, 1H), 1.61 (s, 3H), 1.36 (s, 3H); HPLC (system 1) purity 95%,  $t_{\text{R}} = 9.79$  min. LC–MS (system 2a):  $m/z = 405.6$  ( $\text{M} + \text{H}$ ) $^+$ ,  $t_{\text{R}} = 6.21$  min.

**1,1,1-Trifluoro-4-(5-fluoro-2,3-dihydrobenzofuran-7-yl)-4-methyl-2-(1H-pyrrolo[2,3-c]pyridin-2-ylmethyl)pentan-2-ol (56)**. To a solution of 2-methyl-1H-pyrrolo[2,3-c]pyridine (0.76 mmol) in THF (3 mL) was added *n*-BuLi (2.3 mmol, 2.5 M in hexanes) at  $-78$  °C. After 5 min KO $^t$ Bu (1.5 mmol, 1 M in THF) was added, and the mixture was allowed to warm to room temperature and stirred for 1 h. The green brown suspension was cooled to  $-78$  °C, and **49** (0.35 mmol) in THF (1 mL) was added. The mixture was stirred for 30 min and successively allowed to warm to room temperature. The reaction was quenched with a saturated solution of  $\text{NH}_4\text{Cl}$  (5 mL), extracted with ethyl acetate (3  $\times$  10 mL), and the combined organic layers were dried over  $\text{MgSO}_4$  and concentrated. Flash silica gel chromatography using 0–1% MeOH in  $\text{CH}_2\text{Cl}_2$  gave **56** (7% yield) as a white solid.  $^1\text{H NMR}$  (400 MHz,  $\text{MeOH}-d_4$ )  $\delta$  8.53 (s, 1H), 7.94 (s, 1H), 7.43 (s, 1H), 6.82 (m, 2H), 6.19 (s, 1H), 4.49 (t,  $J = 8.80$  Hz, 2H), 3.06 (m, 2H), 2.91 (d,  $J = 15.16$  Hz, 1H), 2.86 (d,  $J = 15.65$  Hz, 1H), 2.67 (d,  $J = 15.26$  Hz, 1H), 2.09 (d,  $J = 15.08$  Hz, 1H), 1.57 (s, 3H), 1.36 (s, 3H); HPLC (system 1) purity 97%,  $t_{\text{R}} = 9.96$  min. LC–MS (system 2a):  $m/z = 423.5$  ( $\text{M} + \text{H}$ ) $^+$ ,  $t_{\text{R}} = 6.31$  min.

**4-(5-Chloro-2,3-dihydrobenzofuran-7-yl)-1,1,1-trifluoro-4-methyl-2-(1H-pyrrolo[2,3-c]pyridin-2-ylmethyl)pentan-2-ol (57)**. Following the general Boc-deprotection procedure using **54** as a starting material and stirring the mixture for 4 h gave 1-(3-aminopyridin-4-yl)-6-(5-chloro-2,3-dihydrobenzofuran-7-yl)-6-methyl-4-trifluoromethylhept-1-yn-4-ol (assumed yield 100%) as the HCl salt.

Following the general cyclization procedure A starting from 1-(3-aminopyridin-4-yl)-6-(5-chloro-2,3-dihydrobenzofuran-7-yl)-6-methyl-4-trifluoromethylhept-1-yn-4-ol and stirring for 20 h gave **57** (30% yield) as a white solid.  $^1\text{H NMR}$  (400 MHz,  $\text{CDCl}_3$ )  $\delta$  8.64 (s, 1H), 8.07 (d,  $J = 5.76$  Hz, 1H), 7.45 (d,  $J = 5.47$  Hz, 1H), 7.03 (m, 2H), 6.27 (s, 1H), 4.43 (m, 2H), 3.03 (m, 4H), 2.50 (d,  $J = 15.52$  Hz, 1H), 2.40 (d,  $J = 15.52$  Hz, 1H), 1.46 (s, 3H), 1.33 (s, 3H); HPLC (system 1) purity 99%,  $t_{\text{R}} = 10.31$  min. LC–MS (system 2a) = 440.1 ( $\text{M} + \text{H}$ ) $^+$ ,  $t_{\text{R}} = 6.41$  min.

**GR, PR, and MR Binding Assays**. GR, PR, and MR binding assays were performed in a fluorescence polarization microplate format that measures competition for binding to the nuclear receptor between a test compound and a fluorescently labeled receptor ligand or probe. The probes used for the assays were as follows. GR and MR assays: 5 nM tetramethylrhodamine-labeled dexamethasone. PR assay: 5 nM tetramethylrhodamine-labeled RU-486. For GR and MR assays, receptors present in lysates of baculovirus-infected insect cells co-infected with receptor, HSP-70, HSP-90, and p23 were used. For PR binding assays, lysates were generated from insect cells infected with receptor-containing baculovirus alone. Binding reactions consisted of lysate, test compound, and probe combined in assay buffer containing 10 mM TES, 50 mM KCl, 20 mM  $\text{Na}_2\text{MoO}_4 \cdot 2\text{H}_2\text{O}$ , 1.5 mM EDTA, 0.04% w/v CHAPS, 10% v/v glycerol, 1 mM dithiothreitol, pH 7.4. Lysates containing GR, PR, and MR were diluted into the assay 300-fold, 13-fold, and 17-fold into the respective binding reactions. The DMSO concentration in all binding reactions was 1% (v/v). Following 1 h of incubation in the dark at room temperature, fluorescence polarization signal was measured using a Molecular Devices Analyst plate reader with excitation and emission filters of 550 and 580 nm selected and with a 561 nm dichroic mirror installed. Positive control FP signal was measured in assay wells

containing binding reactions without inhibitor. The fluorescence polarization signal produced by maximal inhibition (background control) was determined using the signals from wells containing 2  $\mu\text{M}$  standard inhibitor for each receptor: dexamethasone for GR and MR and RU-486 for PR. Fluorescence polarization signals from duplicate 11-point concentration–response curves were fitted to a four-parameter logistic equation to determine  $\text{IC}_{50}$  values.

**IL-1 Induced IL-6 Assay (Transrepression).** The fibroblast-IL-6 assay measures the ability of test compounds to inhibit the elaboration of IL-6 by human foreskin fibroblasts following stimulation by IL-1 *in vitro*. Human foreskin fibroblasts (ATCC no. CRL-2429) were grown in Iscove's media supplemented with 10% (v/v) charcoal/dextran-treated fetal bovine serum and plated at 20 000 cells/well 2 days prior to assay. On the day of the assay, the media were replaced, followed by the addition of test compound (0.4% DMSO final assay concentration) and recombinant human IL-1 (final concentration = 1 ng/mL). After incubation at 37 °C for 18–24 h, IL-6 in the tissue culture media was quantitated using standard electrochemiluminescence, DELFIA, or ELISA methods. Test compound  $\text{IC}_{50}$  values were determined by fitting the data from duplicate 11-point concentration–response curves to a four-parameter logistic equation. In this assay, IL-6 inhibition is considered a measure of agonist response of the glucocorticoid receptor, and dexamethasone is considered to possess 100% efficacy.

**MMTV Reporter Gene Assay (Transactivation).** HeLa MMTV transactivation assay measures the ability of test compounds to activate MMTV promoter in HeLa cells stably transfected with MMTV luciferase construct. HeLa MMTV cells are grown in DMEM media supplemented with 10% (v/v) fetal bovine serum (Hyclone), 100 U/mL penicillin, 100  $\mu\text{g}/\text{mL}$  streptomycin, 2 mM L-glutamine, 300  $\mu\text{g}/\text{mL}$  Genetecin. The day prior to assay the cells are plated at 25 000 cells/well in 96-well white clear-bottom cell culture plates in DMEM media supplemented with 3% (v/v) FBS, 100 U/mL penicillin, 100  $\mu\text{g}/\text{mL}$  streptomycin, 2 mM L-glutamine. On the day of the assay, the media are replaced, followed by addition of test compound (0.2% DMSO final assay concentration). Positive control wells receive 1  $\mu\text{M}$  dexamethasone and represent 100% induction, while negative control wells receive vehicle only and represent background. After final addition of the compounds, plates are incubated for 6 h at 37 °C and 5%  $\text{CO}_2$ . After the incubation period, luminescence is detected upon cell lysis with Steady-Glo luciferase reagent (Promega no. E2520). Activation of MMTV promoter by test compounds is expressed as percentage relative to positive control. Test compound  $\text{EC}_{50}$  values are determined by nonlinear curve fitting of the data from duplicate eight-point concentration–response curve.

**Aromatase Induction Assay (Transactivation).** The fibroblast-aromatase assay measures the ability of test compounds to induce aromatase activity in human foreskin fibroblasts, as indicated by the production of  $\beta$  estradiol in the presence of exogenously added testosterone. Human foreskin fibroblasts (ATCC no. CRL-2429) were grown in Iscove's media supplemented with 10% (v/v) charcoal/dextran-treated fetal bovine serum and plated at 10 000 cells/well 5 days prior to the assay. On the day of the assay, the media were replaced, followed by the addition of test compound (0.4% DMSO final assay concentration) and testosterone (final concentration = 1  $\mu\text{M}$ ). After incubation at 37 °C for 18–24 h, estradiol was quantitated in the tissue culture media using a commercial ELISA (ALPCO no. 020-DR-2693). Test compound  $\text{EC}_{50}$  values were determined by fitting the data from duplicate 11-point concentration–response curves to a four-parameter logistic equation. For test compound comparison, dexamethasone was considered to possess 100% efficacy in this assay.

**Aromatase Inhibition Assay.** Compounds were evaluated for inhibiting aromatase enzyme using the following aromatase (CYP19) inhibition assay which detects aromatase inhibitors

utilizing recombinant human aromatase (baculovirus/insect cell expressed) and the fluorometric substrate dibenzylfluorescein (DBF). Aromatase metabolizes DBF to fluorescein then gives a fluorescent signal. The assay is conducted in 96-well black, Falcon plate (BD Biosciences, catalog no. 353241) in a total volume of 100  $\mu\text{L}$  per well. Then 40  $\mu\text{L}$  of the cofactor/dilution buffer (1) is added to the plate followed by 10  $\mu\text{L}$  of serially diluted test compounds in duplicate for a final concentration of  $2 \times 10^{-5}$  to  $10^{-9}$  M or 10  $\mu\text{L}$  of phosphate buffer for positive and background control wells. After 10 min of preincubation at 37 °C, the reaction is initiated by adding 50  $\mu\text{L}$  of prewarmed enzyme/substrate mix (see item 2 below) to the test compound wells and positive control wells (maximum activity of CYP19, which represents 100%). The plate is incubated at 37 °C for 30 min. To stop the reaction, 37.5  $\mu\text{L}$  of 2 N NaOH is added to all wells. For background controls, an amount of 50  $\mu\text{L}$  of enzyme/substrate mix (see item 2 below) is added into background control wells. The plate is left at 37 °C incubator for 2 h to develop an adequate signal to background ratio. Fluorescence per well is measured in the fluorescent plate reader. The metabolite concentration is measured using excitation wavelength of 485 nm and emission wavelength of 538 nm. The inhibition of aromatase by test compounds is expressed in percentage relative to positive controls. The  $\text{IC}_{50}$  values for the test compounds are derived from nonlinear curve fitting.

- (1) Cofactor/dilution buffer: 50 mM phosphate buffer, pH 7.4; 1 $\times$  NADPH regenerating system A (20 $\times$  stock, GENTEST, catalog no. 451220); 1 $\times$  NADPH regenerating system B (100 $\times$  stock, GENTEST, catalog no. 451200) and 0.2 mg/mL control protein (insect cell control supersomes, GENTEST, catalog no. 456200).
- (2) enzyme/substrate mix: 50 mM phosphate buffer, pH 7.4, 0.02 nmol/mL human aromatase protein (human CYP19 + P450 reductase supersomes, GENTEST, catalog no. 456260); 0.4  $\mu\text{M}$  dibenzylfluorescein (DBF, GENTEST, catalog no. 451750, prepared at 2 mM in acetonitrile); 0.5 mg/mL control protein (insect cell control supersomes, GENTEST, catalog no. 456200).

**In Vivo LPS-Challenge Assay.** Female Balb/c mice weighing approximately 20 g were used. Mice were administered the test compound and in Cremophor (po) approximately 60 min prior to LPS/D-gal administration. The volume of oral gavage was 0.15 mL. Then mice were administered LPS (*E. coli* LPS 055:85, 1.0  $\mu\text{g}/\text{mouse}$ ) plus D-gal (50 mg/kg) intravenously in 0.2 mL of pyrogen-free saline. One hour after LPS/D-gal, each mouse was anesthetized, bled by cardiac puncture, and collected for serum TNF- $\alpha$  and compound levels. Blood samples were centrifuged at 2500 rpm for 10–15 min, the serum was decanted, and samples were stored frozen at –70 °C until transfer either for TNF- $\alpha$  determination or to Drug Metabolism and Pharmacokinetics for plasma concentration analysis by HPLC. The concentration of TNF- $\alpha$  in the serum was measured by a commercially available ELISA kit (R&D Systems, Minneapolis, MN). ELISA was performed according to the manufacturer's assay procedure. All samples are assayed in duplicate.

**Collagen Induced Arthritis.** Female B10.RIII mice (Jackson Laboratories) were immunized intradermally at 12–15 weeks of age with lyophilized native porcine type II collagen (CII lot P9603, purchased from Dr. Marie Griffiths, Utah University) dissolved overnight at 4 °C in 0.01 N acetic acid at 2 mg/mL. The collagen solution was then emulsified at a 1:1 ratio with complete Freund's adjuvant (containing 2 mg/mL *Mycobacterium tuberculosis* strain H37Ra). On day 0 animals received a single intradermal injection of 100  $\mu\text{L}$  (containing 100  $\mu\text{g}$  of type II collagen) of cold emulsion in the base of the tail. Beginning on day 13 after immunization, all immunized animals were monitored daily for signs of clinical arthritis. Arthritic animals were randomly enrolled into treatment groups until a total of 10 animals per group were achieved. Upon enrollment, the animal



was anesthetized with 50 mg/kg (10 mg/mL) ketamine/15 mg/kg (2 mg/mL) zylazine. A whole body noninvasive density scan was performed to assess body fat content (PIXImus densitometer, Lunar Corp.). At 3–4 h after recovering from anesthesia the animal received the appropriate treatment once a day for a period of 35 days. Disease progression and severity were assessed every Monday, Wednesday, and Friday for 5 weeks. A clinical scoring system was used whereby each limb was graded as follows: 0, normal; 1, erythema and edema in 1–2 digits; 2, erythema and edema in >2 digits or severe edema and erythema encompassing the tarsal and metatarsal joints; 3, edema and erythema encompassing the tarsal and metatarsal joints along with joint deformity. At termination (day 35), a serum sample was collected for biomarker analysis. Triglyceride levels were determined with the Wako L-Type TG-H kit (Wako Diagnostics, Richmond, VA). Free fatty acids in serum were measured using the Wako NEFA-C microtiter procedure (Wako Diagnostics, Richmond, VA, catalog no. 994-75409). For the serum insulin assay, the Ultra Sensitive Rat Insulin ELISA kit (Crystal Chem Inc., Chicago, IL, catalog no. 90060) and mouse insulin standard, 1.28 ng (catalog no. 90090), were used.

**Acknowledgment.** We thank Ronald Magboo, Scott Leonard, and Scott Pennino for their analytical support and Paige Mahaney for proofreading the manuscript.

**Supporting Information Available:** Spectral data for key compounds (**R**)-16 and (**R**)-37. This material is available free of charge via the Internet at <http://pubs.acs.org>.

## References

- Gupta, R.; Jindal, D. P.; Kumar, G. Corticosteroids: the mainstay in asthma therapy. *Bioorg. Med. Chem.* **2004**, *12*, 6331–6342.
- Buttgereit, F.; Saag, K. G.; Cutolo, M.; da Silva, J. A. P.; Bijlsma, J. W. J. The molecular basis for the effectiveness, toxicity, and resistance to glucocorticoids: focus on the treatment of rheumatoid arthritis. *Scand. J. Rheumatol.* **2005**, *34*, 14–21.
- Schäcke, H.; Döcke, W.-D.; Asadullah, K. Mechanisms involved in the side effects of glucocorticoids. *Pharmacol. Ther.* **2002**, *96*, 23–43.
- McMaster, A.; Ray, D. W. Drug insight: selective agonists and antagonists of the glucocorticoid receptor. *Nat. Clin. Pract. Endocrinol. Metab.* **2008**, *4*, 91–101.
- (a) Zhou, J.; Cidlowski, J. A. The human glucocorticoid receptor: one gene, multiple proteins and diverse responses. *Steroids* **2005**, *70*, 407–417. (b) Adcock, I. M. Molecular mechanisms of glucocorticosteroid actions. *Pulm. Pharmacol. Ther.* **2000**, *13*, 115–126. (c) Heck, S.; Kullmann, M.; Gast, A.; Ponta, H.; Rahmsdorf, H. J.; Herrlich, P.; Cato, A. C. B. A distinct modulating domain in glucocorticoid receptor monomers in the repression of activity of the transcription factor AP-1. *EMBO J.* **1994**, *13*, 4087–4095. (d) Katzenellenbogen, J. A.; Katzenellenbogen, B. S. Nuclear hormone receptors: ligand-activated regulators of transcription and diverse cell responses. *Chem. Biol.* **1996**, *3*, 529–536.
- (a) Resche-Rigon, M.; Gronemeyer, H. Therapeutic potential of selective modulators of nuclear receptor action. *Curr. Opin. Chem. Biol.* **1998**, *2*, 501–507. (b) Barnes, P. J. Anti-inflammatory actions of glucocorticoids: molecular mechanisms. *Clin. Sci.* **1998**, *94*, 557–572. (c) Buckbinder, L.; Robinson, R. P. The glucocorticoid receptor: molecular mechanism and new therapeutic opportunities. *Curr. Drug Targets: Inflammation Allergy* **2002**, *1*, 127–136. (d) Burnstein, K. L.; Cidlowski, J. A. The down side of glucocorticoid receptor regulation. *Mol. Cell. Endocrinol.* **1992**, *83*, C1–C8.
- Reichardt, H. M.; Tuckermann, J. P.; Göttlicher, M.; Vujic, M.; Weih, F.; Angel, P.; Herrlich, P.; Schütz, G. Repression of inflammatory responses in the absence of DNA-binding by the glucocorticoid receptor. *EMBO J.* **2002**, *20*, 7168–7173.
- (a) Schäcke, H.; Berger, M.; Hansson, T. G.; McKerrecher, D.; Rehwinkel, H. Dissociated non-steroidal glucocorticoid receptor modulators: an update on new compounds. *Expert Opin. Ther. Pat.* **2008**, *18*, 339. (b) Hudson, A. R.; Roach, S. L.; Higuchi, R. I. Recent developments in the discovery of selective glucocorticoid receptor modulators (SGRMS). *Curr. Top. Med. Chem.* **2008**, *8*, 750–765. (c) Regan, J.; Razavi, H.; Thomson, D. Advances toward Dissociated Non-Steroidal Glucocorticoid Receptor Agonists. *Annual Reports in Medicinal Chemistry*; Doherty, A. M., Ed.; Academic Press: New York, 2008; Vol. 43, pp 141–154. (d) Mohler, M. L.; He, Y.; Wu, Z.; Hong, S.-S.; Miller, D. D. Dissociated non-steroidal glucocorticoids: tuning out untoward effects. *Expert Opin. Ther. Pat.* **2007**, *17*, 37. (e) Robinson, R. P.; Buckbinder, L.; Haugeto, A. I.; McNiff, P. A.; Millham, M. L.; Reese, M. R.; Schaefer, J. F.; Yocum, S. A. Octahydrophenanthrene-2,7-diol analogues as dissociated glucocorticoid receptor agonists: discovery and lead exploration. *J. Med. Chem.* **2009**, *52*, 1731–1743. (f) Berlin, M. Recent advances in the development of novel glucocorticoid receptor modulators. *Expert Opin. Ther. Pat.* **2010**, *20*, 855–873.
- Manuscript in preparation. Bekkali, Y.; Betageri, R.; Emmanuel, M. J.; Hammach, A.; Harcken, H. J.; Kirrane, T. M.; Kuzmich, D.; Lee, T. W.; Liu, P.; Patel, U. R.; Razavi, H.; Riether, D.; Takahashi, H.; Thomson, D. S.; Wang, J.; Zindell, R.; Proudfoot, J. R. Preparation of Hydroxytrifluoromethyl-alkylpyrrolopyridines, -indoles, and Related Compounds as Modulators of Glucocorticoid Receptor Function. WO 2005030213, 2005.
- (a) Regan, J.; Lee, T. W.; Zindell, R. M.; Bekkali, Y.; Bentzien, J.; Gilmore, T.; Hammach, A.; Kirrane, T. M.; Kukulka, A. J.; Kuzmich, D.; Nelson, R. M.; Proudfoot, J. R.; Ralph, M.; Pelletier, J.; Souza, D.; Zuvella-Jelaska, L.; Nabozny, G.; Thomson, D. S. Quinol-4-ones as steroid A-ring mimetics in nonsteroidal dissociated glucocorticoid agonists. *J. Med. Chem.* **2006**, *49*, 7887–7896. (b) Kuzmich, D.; Kirrane, T.; Proudfoot, J.; Bekkali, Y.; Zindell, R.; Beck, L.; Nelson, R.; Shih, C.-K.; Kukulka, A. J.; Paw, Z.; Reilly, P.; Deleon, R.; Cardozo, M.; Nabozny, G.; Thomson, D. Identification of dissociated non-steroidal glucocorticoid receptor agonists. *Bioorg. Med. Chem. Lett.* **2007**, *17*, 5025–5031.
- (a) Schäcke, H.; Schottelius, A.; Döcke, W.-D.; Strehlke, P.; Jaroch, S.; Schmees, N.; Rehwinkel, H.; Hennekes, H.; Asadullah, K. Dissociation of transactivation from transrepression by a selective glucocorticoid receptor agonist leads to separation of therapeutic effects from side effects. *Proc. Nat. Acad. Sci. U.S.A.* **2004**, *101*, 227–232. (b) Jaroch, S.; Rehwinkel, H.; Schäcke, H.; Schmees, N.; Skuballa, W.; Schneider, M.; Hubner, J.; Petrov, O. 5-Substituted Quinoline and Isoquinoline Derivatives, a Method for the Production Thereof and Their Use as Antiproliferatives. PCT Int. Appl. WO20050998, 2006. (c) Biggadike, K.; Boudjelal, M.; Clackers, M.; Coe, D. M.; Demaine, D. A.; Hardy, G. W.; Humphreys, D.; Inglis, G. G. A.; Johnston, M. J.; Jones, H. T.; House, D.; Loiseau, R.; Needham, D.; Skone, P. A.; Uings, I.; Veitch, G.; Weingarten, G. G.; McLay, I. M.; Macdonald, S. J. F. Nonsteroidal glucocorticoid agonists: Tetrahydronaphthalenes with alternative steroidal A-ring mimetics possessing dissociated (transrepression/transactivation) efficacy selectivity. *J. Med. Chem.* **2007**, *50*, 6519–6534.
- GLIDE, version 5.0; Schrödinger LLC: New York, 2008.
- Bledsoe, R. K.; Montana, V. G.; Stanley, T. B.; Delves, C. J.; Apolito, C. J.; McKee, D. D.; Conlser, T. G.; Parks, D. J.; Stewart, E. L.; Willson, T. M.; Lambert, M. H.; Moore, J. T.; Pearce, K. H.; Xu, H. E. Crystal structure of the glucocorticoid receptor ligand binding domain reveals a novel mode of receptor dimerization and coactivator recognition. *Cell* **2002**, *110*, 93–105.
- (a) Kelly, T. A.; Patel, U. R. *J. Org. Chem.* **1995**, *60*, 1875. (b) Park, S. S.; Choi, J.-K.; Yum, E. K.; Ha, D.-C. A facile synthesis of 2,3-disubstituted pyrrolo[2,3-b]pyridines via palladium-catalyzed heteroannulation with internal alkenes. *Tetrahedron Lett.* **1998**, *39*, 627–630. (c) Crous, R.; Dywer, C.; Holzapfel, C. W. Cross coupling strategies towards the synthesis of the streptogramin CD moiety. *Heterocycles* **1999**, *51*, 721. (d) Kadnikov, D. V.; Larock, R. C. Synthesis of 2-quinolones via palladium-catalyzed carbonylative annulation of internal alkenes by N-substituted o-iodoanilines. *J. Org. Chem.* **2004**, *69*, 6772–6780. (e) Venuti, M. C.; Stephenson, R. A.; Alvarez, R.; Bruno, J. J.; Strosberg, A. M. Inhibitors of cyclic AMP phosphodiesterase. 3. Synthesis and biological evaluation of pyrido and imidazolyl analogues of 1,2,3,5-tetrahydro-2-oxoimidazo[2,1-b]quinazoline. *J. Med. Chem.* **1988**, *31*, 2136.
- Lee, T. W.; Proudfoot, J. R.; Thomson, D. S. A concise asymmetric route for the synthesis of a novel class of glucocorticoid mimetics containing a trifluoromethyl-substituted alcohol. *Bioorg. Med. Chem. Lett.* **2006**, *16*, 654–657.
- Harcken, C.; Ward, Y.; Thomson, D.; Riether, D. A general and efficient synthesis of azaindoles and diazaindoles. *Synlett* **2005**, *20*, 3121–3125.
- Waage, A.; Slupphaug, G.; Shalaby, R. Glucocorticoids inhibit the production of IL6 from monocytes, endothelial cells and fibroblasts. *Eur. J. Immunol.* **1990**, *20*, 2439–2443.
- (a) Bourguet, W.; Germain, P.; Gronemeyer, H. Nuclear receptor ligand-binding domains: three-dimensional structures, molecular interactions and pharmacological implications. *Trends Pharmacol. Sci.* **2000**, *21*, 381–388. (b) Bledsoe, R. K.; Stewart, E. L.; Pearce, K. H.

- Structure and function of the glucocorticoid receptor ligand binding domain. *Vitam. Horm.* **2004**, *68*, 49–91.
- (19) (a) Madauss, K. P.; Bledsoe, R. K.; McLay, I.; Stewart, E. L.; Uings, I. J.; Weingarten, G.; Williams, S. P. The first X-ray crystal structure of the glucocorticoid receptor bound to a non-steroidal agonist. *Bioorg. Med. Chem. Lett.* **2008**, *18*, 6097–6099.  
(b) Biggadike, K.; Bledsoe, R. K.; Hassell, A. M.; Kirk, B. E.; McLay, I. M.; Shewchuk, L. M.; Stewart, E. L. X-ray crystal structure of the novel enhanced-affinity glucocorticoid agonist fluticasone furoate in the glucocorticoid receptor–ligand binding domain. *J. Med. Chem.* **2008**, *51*, 3349–3352.
- (20) Compound **37** was tested in an aromatase inhibition assay and showed an  $IC_{50}$  of  $0.07 \mu\text{M}$ . In the aromatase induction assay, no increase in aromatase levels was observed, and thus, it was concluded that despite the ability of **37** to inhibit aromatase, the compound does not induce it.